ALEXANDER, SYMONE A., M.S. Diastereoselective Cyclization of Lactones via Brønsted Acid Catalysis. (2020)
Directed by Dr. Kimberly Petersen. 46 pp.

Chiral molecules play a vital role in supporting biologically effective drugs. Consequently, a majority of pharmaceutical companies seek to isolate the enantiomers of molecules in drug design. Enantioselective synthesis can be a valuable tool for creating single enantiomers. A particular technique for synthesizing enantiomers is desymmetrization, where a prochiral molecule loses its symmetry elements through a reaction. In this work, desymmetrization will be done utilizing a diester with a Brønsted acid catalyst, to achieve mild reaction conditions for cyclization. Providing these mild conditions decreases the chances of side reactions which can happen in harsher reaction conditions hindering enantioselectivity. This approach of using organocatalysts to perform these cyclizations is novel given cyclizations of this nature typically utilize transition metal catalysts.

This thesis describes the expansion of previous work in the Petersen Group in the synthesis of six-membered lactones with multiple stereocenters. Previous work utilized prochiral nitrile compounds to synthesize δ-lactones, and this work provides the results of diastereo- and enantioselective desymmetrizations with malonic esters. Once cyclization was achieved the reaction was optimized by varying the achiral Brønsted acid catalyst used, the temperature, and solvents. After optimization of our first substrate containing a bulky phenyl group, a second less bulky alkylating agent was used to examine the diastereoselectivity of this new multicentered compound.

DIASTEREOSELECTIVE CYCLIZATION OF LACTONES VIA BRØNSTED ACID CATALYSIS

by

Symone A. Alexander

A Thesis Submitted to
the Faculty of The Graduate School at
The University of North Carolina at Greensboro
in Partial Fulfillment
of the Requirements for the Degree
Master of Science

Greensboro
2020

Approved by

_____
Committee Chair

To my family which has supported me through this academic journey, especially my mother Staci Alexander, and my Aunt Sherry and Uncle William (Taylor), I thank you from the bottom of my heart for all of the love and support you have given me. To all of my friends, both old and new, I could not have done this without you and to all of my colleagues you have helped me get me through this more than you can imagine and my gratitude is immeasurable

APPROVAL PAGE

This thesis written by Symone A. Alexander has been approved by the following committee of the Faculty of The Graduate School at The University of North Carolina at Greensboro.

Committee Chair _____

Committee Members _____

_____

_____

Date of Acceptance by Committee

_____

Date of Final Oral Examination

TABLE OF CONTENTS

Page

LIST OF TABLES

Page

LIST OF FIGURES

Page

CHAPTER I

INTRODUCTION

I.1 Stereochemistry

The use of small organic molecules in the synthesis of pharmaceuticals and natural products has been a long developing field. Almost two centuries ago, the phenomenon of chirality was discovered and its function in not only biology, but in chemical and pharmaceutical production continues to be studied.[1] Derived from the Ancient Greek word, *cheir,* which relates to handedness, chirality of molecules is defined by an inability of two mirror image molecules to be superimposable. A pair of non-superimposable mirror images are called enantiomers. Typically the point of chirality will be a carbon atom with four different substituents attached. This center can be referred to as a stereocenter and how the substituents are attached will determine the configuration of an enantiomer. With the addition of multiple stereocenters, molecules that have opposing absolute configurations at each center can still be enantiomers (e.g. **A** and **B** or **C** and **D** in Figure 1),

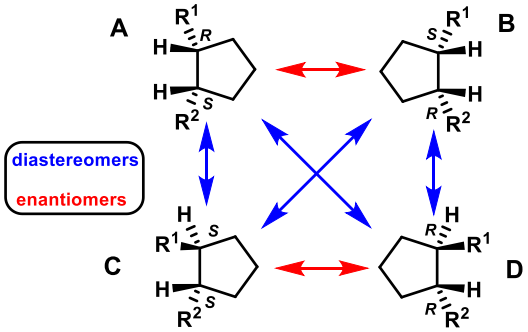

Figure 1. Differences between enantiomers and diastereomers

but will become diastereomers when at least one of those stereocenters retains the same absolute configuration (e.g. **A** and **C**, **A** and **D, B** and **C**, **B** and **D** in Figure 1). While enantiomers have indistinguishable physical properties, they can be differentiated by how they react with polarized light and other enantioenriched molecules. Diastereomers, alternatively, can have varying chemical and even physical properties that help distinguish between them. More importantly enantiomers and diastereomers can exhibit varying biological effects. In 1933, Easson and Stedman proposed a three-point interaction of a drug with a receptor site which in many cases will allow for the drug to show a specific activity within the body.[1] Because of this, the research into chiral drugs, specifically the synthesis of enantiomerically pure drugs is a high priority for many pharmaceutical companies. Thus, drugs that exhibit bioactivity often have at least one chiral center. Seen in a variety of synthetic and naturally occurring compounds, the *R* or *S* derivatives can have wildly differing biological effects based on chemical site receptors. For instance, the drug methadone is "a central-acting analgesic with a high affinity for μ-opioid receptors."[1] This drug typically is used as a racemic (or 1:1 mixture of enantiomers) drug, though the *R* enantiomer has been shown to be almost 25-50 fold more effective than the *S* enantiomer (Figure 2).

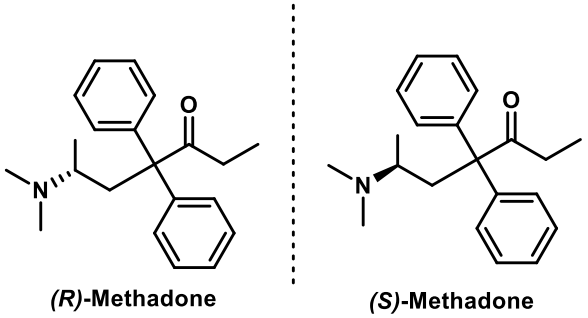

***(R)*-Methadone** ***(S)*-Methadone**

Figure 2. Methadone enantiomers

The prevalence of the racemic drug over the enantiopure drug in the treatment of patients is associated with cost as it is cheaper to synthesize the racemate rather than isolate the *R* enantiomer. At the same time, synthesizing enantiopure compounds allows pharmaceutical companies the ability to study the bioactivity of one enantiomer over another for maximum benefits as well as avoid potential adverse effects.[2] A particular compound of interest is the lactone motif, which can be found throughout nature and serves as a building block to many larger structures. One specific example of a naturally occurring substance with a δ-lactone motif are coumarins (Figure 3), especially those with a 3,4-dihyrdocoumarin core structure.[18]

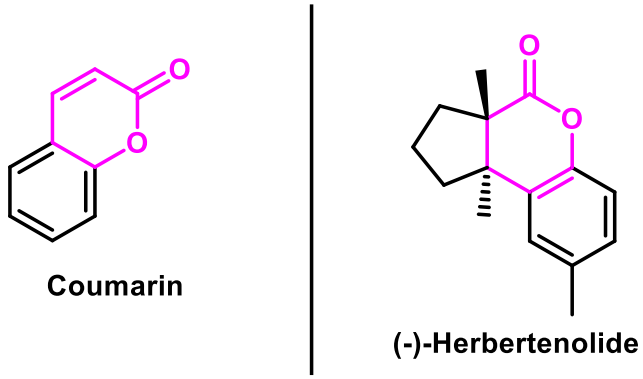

Figure 3. Base structure for coumarin and a coumarin derivative

Some coumarin derivatives, like (-)-Herbertenolide (Figure 3) have been found to exhibit growth suppression of certain pathogenic plant fungi.[19] δ-Lactones, or δ-valerolactones, are not just useful as building blocks for other compounds but also have been deemed especially important for the production of biodegradable polymers. Currently poly(ethylene glycol), PEG, has been the most widely used polyether in the biomedical field.[8,12] However, along with its many biomedical and chemical uses, the nonbiodegradability of PEG has been seen as an increasing concern. Poly(δ-

valerolactones) along with poly(ε-caprolactones) are aliphatic polyesters that can be synthesized from the polymerization of δ-valerolactones and ε-caprolactones, respectively. These polymers are unique in that they are more biodegradable, have low cytotoxicity, and good "permeability to a wide variety of drugs,"[8] which makes them more viable candidates for PEG analogs. One particular route of polymerization of δ-valerolactones has been the controlled ring-opening polymerization (ROP) utilizing functionalized lactones (Figure 4).[12]

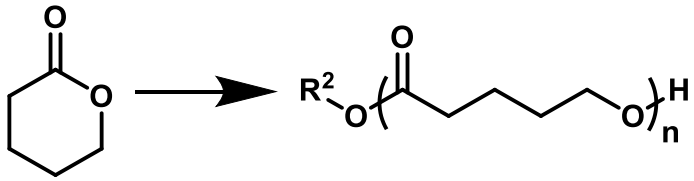

Figure 4. Ring-opening polymerization (ROP) of δ-valerolactones

It was found that functionalized lactones serve as a valuable portion of this ROP methodology though the syntheses to prepare the monomers was "cumbersome" and required many steps.[13] It was even seen in the work done by Li and associates that the thiol-ene adducts of exocyclic unsaturated δ-valerolactones were more stable than the endocyclic unsaturated δ-valerolactones used in prior work.[12] The cyclic lactones synthesized by the Petersen group could then serve as facile starting material for ROP strategies along with serving as potential building blocks for enantiopure drugs. The added value of chirality to polyesters has been shown in the production of poly(hydroxy acid)s. Poly(hydroxy acid)s can be synthesized from the ring-opening polymerization of β-and γ-lactones as well as lactides and *O*-carboxyanhydrides, and the backbones of

these polymers contain varying side chain groups that depending on their tacticity can "modulate the physical, mechanical, and biological properties of the resulting polymer."[7]

I.2 Asymmetric Synthesis

When chiral compounds are synthesized, there is the potential for the products to result in either a racemic mixture (an equal production of both the *R* and *S* enantiomers) or a mixture of enantiomers with enantiomeric excess (ee), where there is a higher percentage of either the *R* or *S* enantiomer. This selectivity can also be seen for diastereomers with varying ratios, or diastereomeric ratios (dr). Enantiomeric or diastereomeric ratios can be determined through a variety of chromatographic techniques. As diastereomers contain differing chemical properties, they can often be separated using standard chemical techniques such as crystallization or chromatography. Enantiomers, however, have identical physical properties, and thus must be separated utilizing enantioselective methodologies like chiral liquid chromatography or kinetic resolution.

During kinetic resolution, a chiral reagent or catalyst, will promote the reaction of a specific enantiomer over the other due to differing reaction rates. While kinetic resolution is useful in synthesizing one enantiomeric product over the other, because reactions are performed using a racemic mixture, only half the starting material would be successfully converted into product (Figure 5) resulting in, at best, a 50% yield.

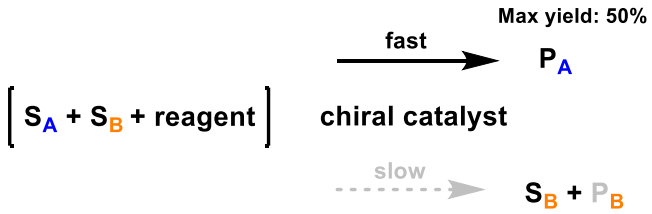

Figure 5. Theoretical kinetic resolution

This can still be advantageous as the remaining enantioenriched starting material can then be used to synthesize other enantiomeric products. The use of organocatalysts for asymmetric synthesis is useful as they are relatively non-toxic and more environmentally sustainable compared to transition metal catalysts. The Petersen lab has employed the desymmetrization of malonic esters to synthesize lactone derivatives (Figure 6).[3]

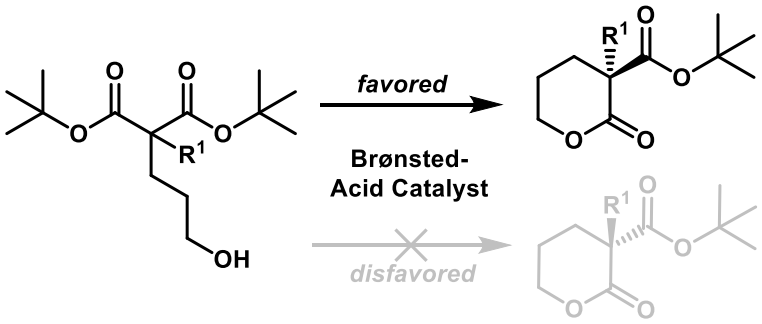

Figure 6. Theoretical desymmetrization cyclization of malonic esters

As the malonic esters are symmetric at the central carbon before cyclization, organocatalysts, specifically chiral catalysts, induce a desymmetrization of the ester. This encourages enantioenrichment of the resulting lactone as the activation energy for a specific enantiomer would be lowered. This allows for the more favored synthesis of one conformation over the other as seen in Figure 6.

I.3 Brønsted acid catalysts

The use of a Brønsted acid to drive the intramolecular cyclization has proved to be quite efficient and has the advantages of being “easy to handle and generally stable toward oxygen and water” while also having a relatively long shelf life.[4] Some organocatalysts used in the Petersen lab have included *p*-toluenesulfonic acid, methylsulfonic acid, trifluoroacetic acid, and the axially chiral 3,3’-Bis(2,4,6-triisopropylphenyl)-1,1’binaphthyl-2,2’-diylhydrogen phosphate (TRIP catalyst), as seen in Figure 7.

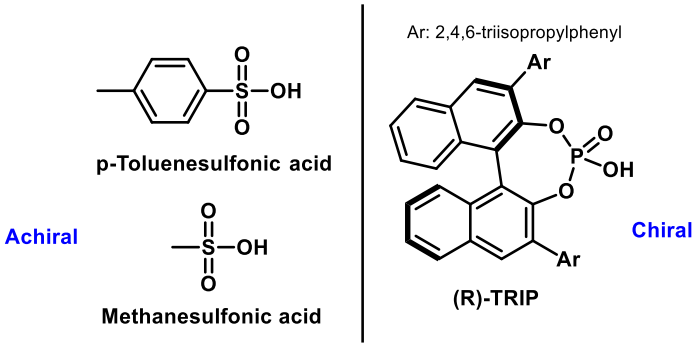

Figure 7. Brønsted acid catalysts

The TRIP catalyst in particular has shown favorable results in the enantioselective desymmetrization of malonic esters to synthesize lactone derivatives. While *p*-Toluenesulfonic acid, methylsulfonic acid, and trifluoroacetic acid can be used to cyclize the malonic esters, they produce racemates. Of the possible Brønsted acid catalysts that can be used to generate enantioenriched lactones, chiral phosphoric acids have shown the most promise for the Petersen group. As seen in Figure 8, the phosphoryl oxygens act as the Brønsted acid/base sites for hydrogen bonding interactions.

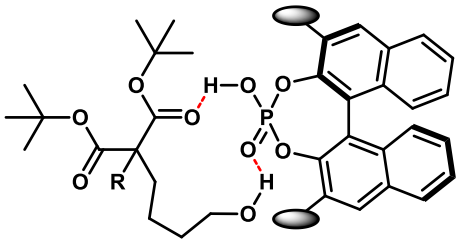

Figure 8. Proposed activation complex

These hydrogen bonds serve to initiate a complex formation between the chiral Brønsted acid and the ester carbonyl group and the hydroxyl end group of the malonic ester. The electrophilic carbon atom of the ester group can then easily undergo nucleophilic attack by the oxygen atom of the hydroxyl group for cyclization (Figure 9).[10]

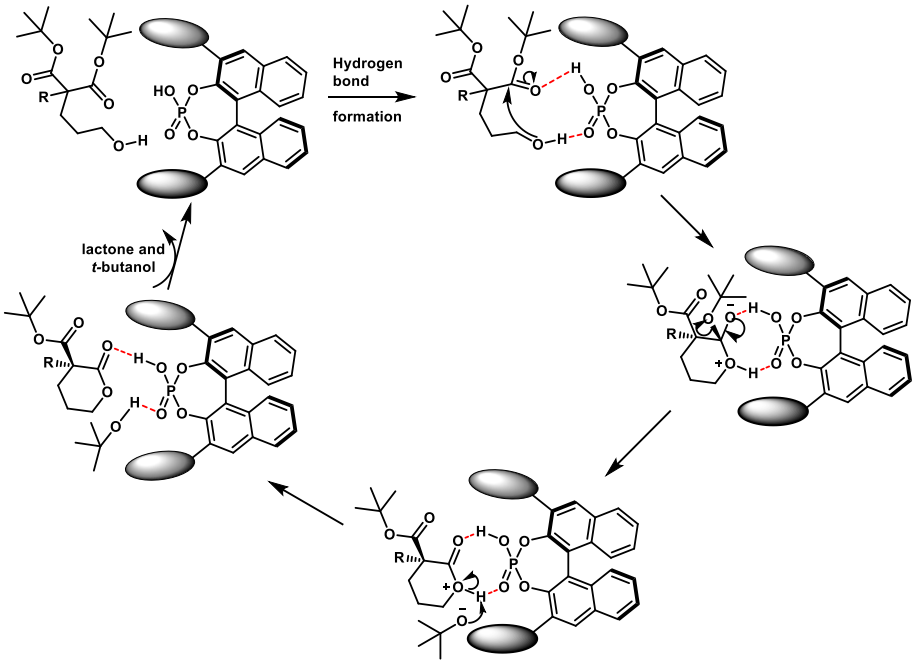

Figure 9. Proposed mechanism for cyclization

The potential enantioselectivity of these Brønsted acids, particularly for 1,1'-bi-2-naphthol (BINOL) phosphoric acids (Figure 10), is then influenced not only by the ring system, but also the substituents attached to that ring system.

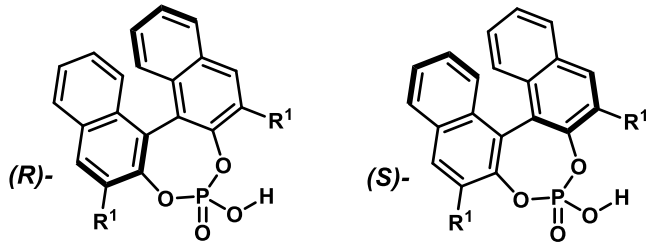

Figure 10. Structure of BINOL phosphoric Brønsted acids

For phosphoric acid catalysts, ring systems not only "restrict the conformational flexibility of the chiral backbone," but the substituents added to that ring system serve to act as substrate recognition site due to the dual Brønsted acid/base sites of the phosphoric acid and "the steric and electronic influence of the substituents."[17]

I.4 Previous Work of the Petersen Group

As alluded to before, this research utilized the novel asymmetric synthesis technique developed by Dr. Jennifer Wilent of the Petersen group, who employed prochiral compounds, specifically malonic esters, to produce *R* or *S* lactone derivatives

from desymmetrization.[3] The primary compounds synthesized in this work were γ-lactones in high yields and enantioenrichment (Figure 11).

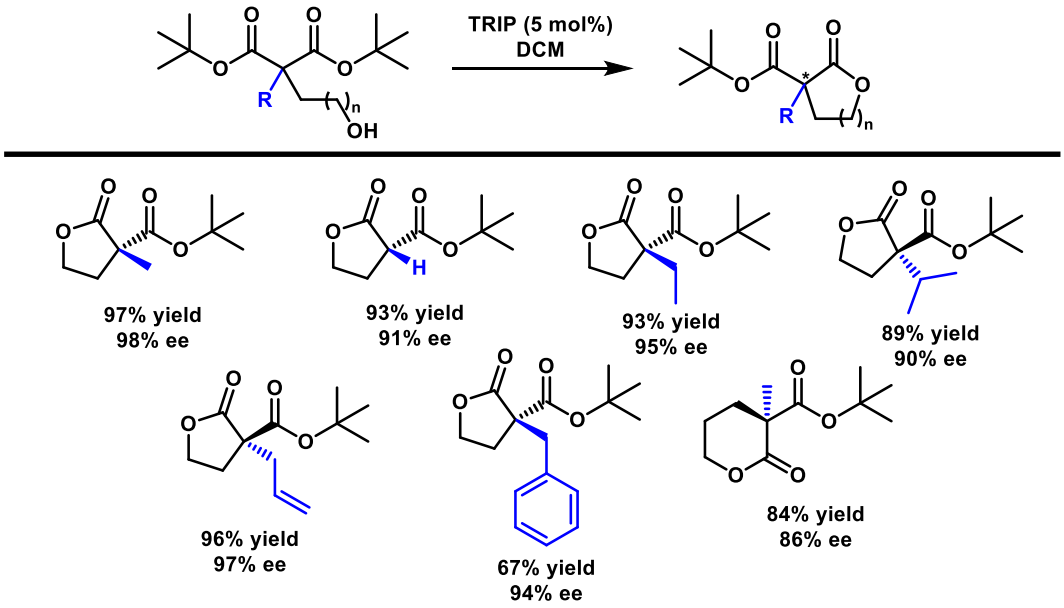

Figure 11. Results from work by Dr. Wilent[3]

Utilizing Dr. Wilent's work, Dr. Amber Kelley and a PhD student Rhashanda Haywood sought to further examine the use of cyclic substrates in lactone synthesis particularly for the synthesis of coumarin derivatives. The 3,4-dihydrocoumarin derivatives produced from these reactions were prepared in moderate to high yields and the addition of a secondary alkyl group to the center of a malonic ester did not display a great decrease in ee with increased steric size (Figure 12). The 3,4-dihydrocoumarin derivatives with all carbon quaternary center were found to have not only the highest yields, but also the best ee.[18]

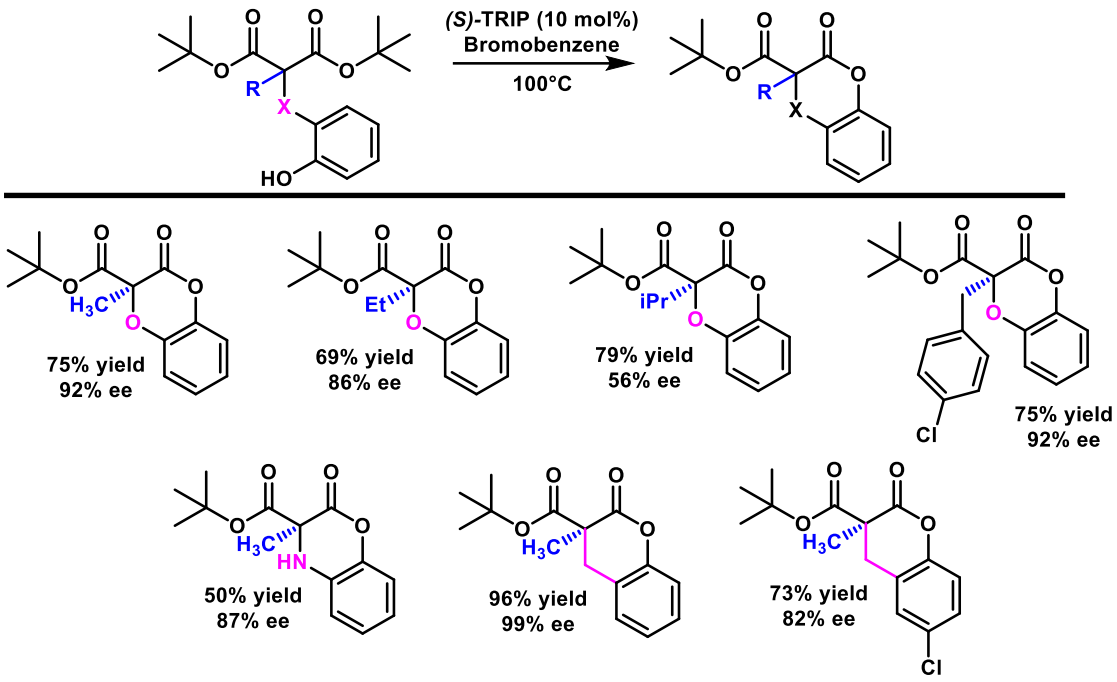

Figure 12. Results of Coumarin derivative synthesis

Building from the work done by Dr. Wilent, Dr. Ghassan Qabaja was able to synthesize lactones from α, β- and α, γ-disubstituted hydroxy esters through a kinetic resolution to produce enantioenriched lactone derivative diastereomers (for a select example see Figure 13).[11] These kinetic reactions were found to favor a "dicoordination model" wherein the energy profiles of the most selective cyclization and its diastereomer were calculated and compared. The barrier heights for the most selective kinetic resolution were found and the more favored diastereomer was determined to have lower barriers for activation which likely allow for its favorable selectivity.

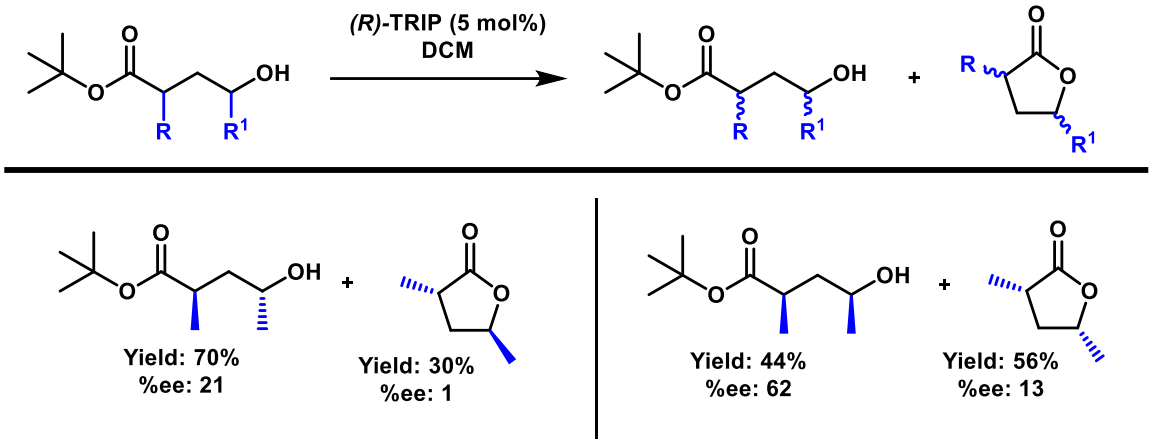

Figure 13. Results from Dr. Qabaja[11]

Racemic cyclic hydroxy esters were also analyzed in this research and were found to be better kinetic resolution substrates and "more selective due to the conformational restriction that places the alcohol in closer proximity to the ester, giving a more rigid transition state."[11] Having a cyclic system that connected the R and R^1 substituents not only shifted the hydroxyl terminal group closer to the ester on the ring system, but also inverted its position to an internal point in the compound (Figure 14), allowing for greater selectivity for all of the substrates that were observed.

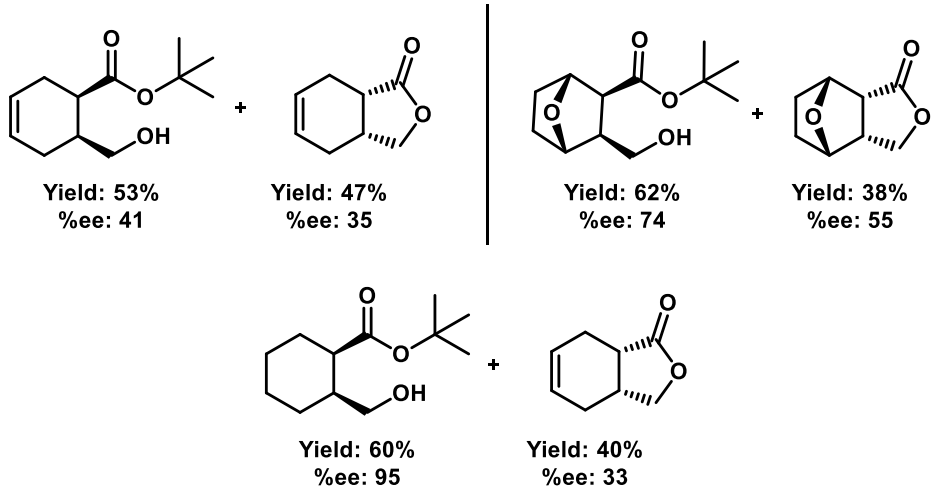

Figure 14. A sample of the results for racemic cyclic hydroxy esters[11]

While the synthesis of γ-lactones tends to have more prevalence than δ-lactones and it has been theorized that 5 membered ring lactones have a greater ease for cyclization than 6 membered ring lactones. This is likely due to the ring conformations seen in δ-lactones, which typically favors the higher energy half-chair and boat conformations, while γ-lactones favor the lower energy envelope conformation.[6] The focus on the synthesis of δ-lactones with multiple stereocenters, creates the opportunity to first generate δ-lactones with high diastereomeric ratios utilizing achiral Brønsted acids, and then single enantiomers by using chiral organocatalysts. Additionally by utilizing an organocatalyst, these cyclizations can be done in a milder, more stable, and more environmentally friendly conditions. The use of chiral Brønsted acid organocatalysts to cyclize symmetric diesters makes the work described in this thesis quite novel as most cyclizations of this nature have been done employing transition metal catalysts, like Platinum (Pt) or Titanium (Ti).[23,24] Additionally, the work in this thesis will be novel for the Petersen group as the synthesis of diastereomeric lactones had not been accomplished utilizing diesters.

Moreover, ROP with disubstituted δ-lactones has been less commonly studied, but the substitution to the lactone ring has been shown to "significantly affect" the polymerization of δ-lactones.[16] Also based on the work done with poly(hydroxy acid)s, the varying properties of these different enantiomeric and diastereomeric δ-lactones could then be studied to generate novel polymers. Thus allowing for future collaborations with groups looking to synthesize these types of polymers.

CHAPTER II

DIASTEREOSELECTIVE DESYMMETRIZATIONS OF DIESTERS

II.1 Present Work

Building from the work published in *ChemistrySelect* by Dr. Kelley et al. regarding the synthesis of 3,4-Dihydrocoumarins[18] as well as the work done by Dr. Qabaja with asymmetric synthesis of hydroxy esters with multiple stereocenters, this project seeks to show the processes developed for synthesizing δ-lactone diastereomers through the desymmetrization of malonic esters (Figure 15).

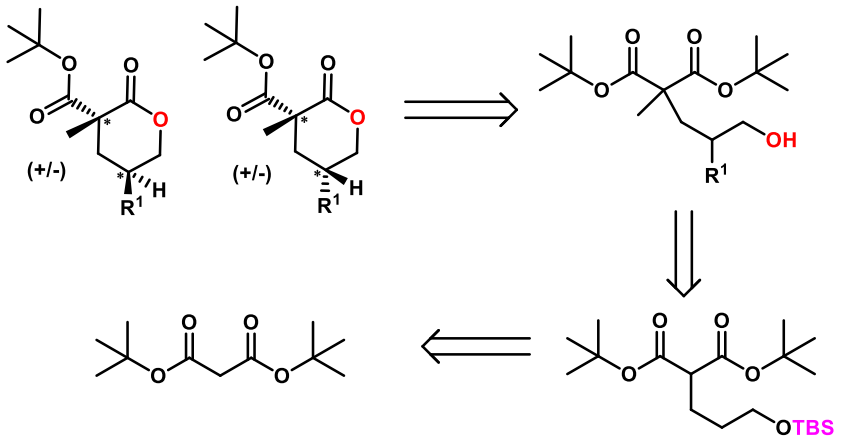

Figure 15. Retrosynthesis of diastereomers

As alkylating agents with a second chiral center were not commercially available, they needed to be synthesized. A method for synthesizing a monosubstituted alkylating group that had a protected hydroxy group had been previously developed in the Petersen group (Figure 16).

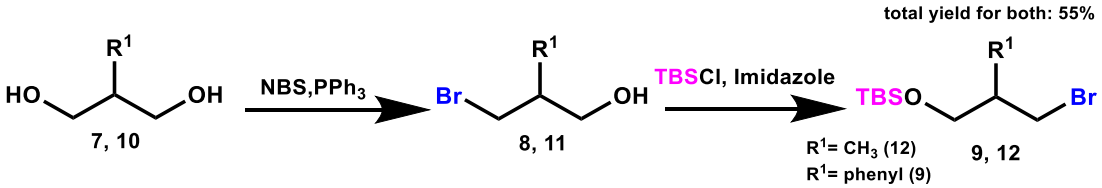

Figure 16. General method for alkylating agent synthesis

Thus starting with 2-phenyl-1,3-pronanediol, **7**, and 2-methyl-1,3-propanediol, **10**, these diols underwent monobromination by an Appel reaction. This addition of bromide produced compounds **8** and **11**, with this new substituent acting as a more efficient leaving group for later substitution with any malonic ester. Next, to prevent any premature cyclization, the remaining unsubstituted hydroxyl group was protected with *t*-butyldimethylsilylchloride (TBS-Cl) to obtain substituted (3-bromopropoxy)-*tert*-butyldimethylsilanes, **9** and **12**. However, the TLC visualization process was near impossible for purification of compounds **11** and **12**, so alkylation had to be done immediately after the synthesis.

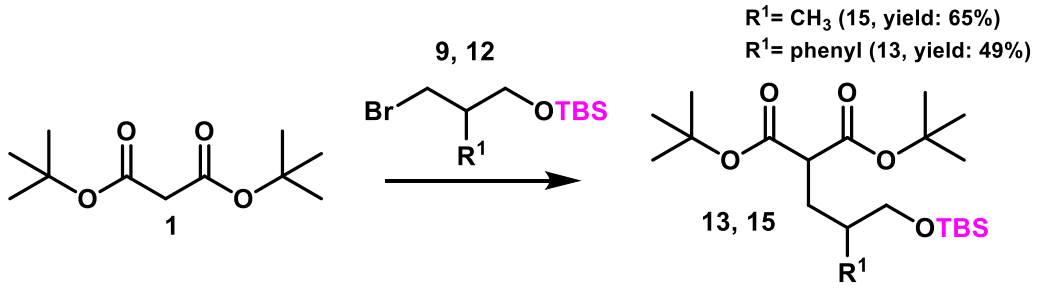

Figure 17. Alkylation with secondary stereocenter

Once these alkylating agents were created, they were added to the central carbon of a di-*tert*-butyl malonate, **1** (Figure 17). Prior work performing this alkylation had been done by adding the alkylating agent to the malonate **1** in a 0°C ice bath with sodium hydride and then allowing the reaction to warm to room temperature. Initially this same

procedure was followed employing compound **9** as an alkylating agent that gave yields ranging from 4-33%, with a 33% yield occurring when the reaction was given a week to stir at room temperature. By modifying the reaction to warming the mixture slightly to room temperature after the addition of the malonate and the alkylating agent the flask was then heated to 70°C in an oil bath. This allowed yields to almost double. As **12** does not have the same bulky benzene ring attached at the second carbon, the initial methodology for alkylation with sodium hydride in THF was performed with compound **1**, without the need for heat to push the reaction forward.

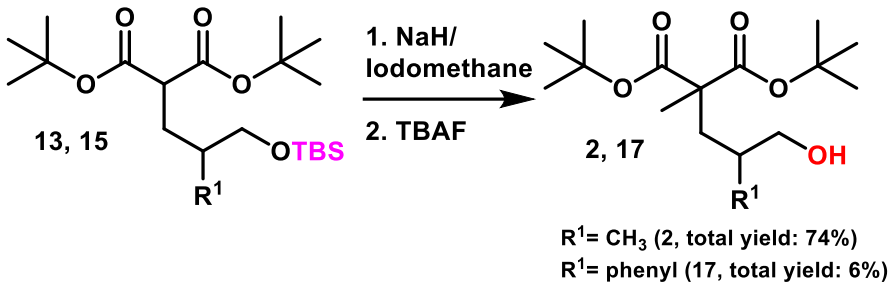

Figure 18. Formation of the cyclization starting material

Once this first alkylation was completed compounds **13** and **15** underwent a second alkylation with iodomethane to produce fully alkylated products **14** and **16**. The tert-butyldimethylsilane protecting group was then removed with tetra-n-butylammonium fluoride (TBAF) to reveal the hydroxy group for compounds **2** and **17** (Figure 18). Compound **2** was cyclized (Figure 19) with three different achiral Brønsted acid catalysts (Table 1), *p*-Toluenesulfonic acid (p-TsA), methylsulfonic acid (MsOH), and trifluoroacetic acid (TFA) to optimize the diastereoselectivity of the reaction.

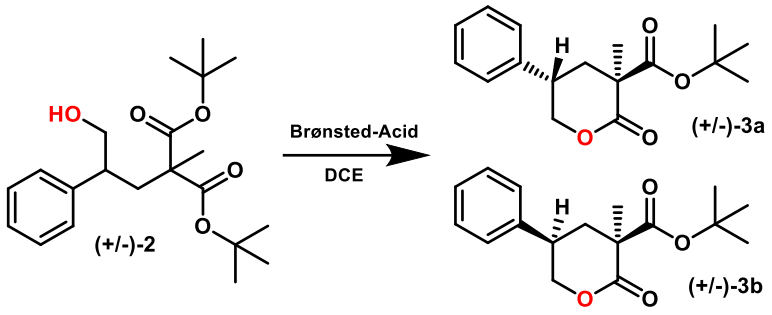

Figure 19. Achiral Brønsted acid cyclization screen

Table 1. Achiral Brønsted acid screen

Entry	Catalyst	Yield (%)	dr
1	p-TsA	70	1:4
2	MsOH	39	3:1
3	TFA	53	1:5

The acid catalyst screen showed that the p-TsA had the best yields, but TFA had the best diastereoselectivity (entry 1 and 3, Table 1). Though the TFA did have better dr than the p-TsA, the p-TsA was chosen due to its structural similarity to the chiral TRIP catalyst. From these results, further optimization was completed by changing the reaction temperatures and solvent (Figure 20).

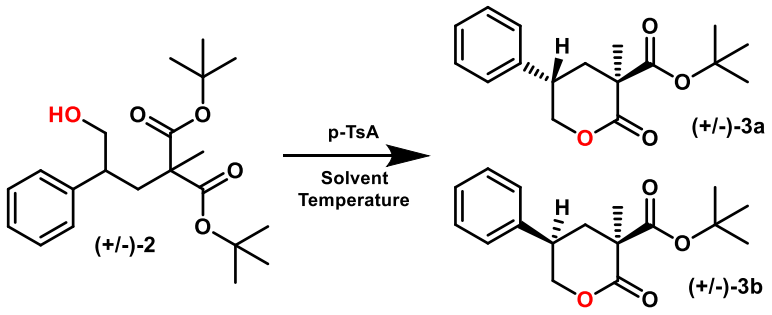

Figure 20. p-TsA optimization screen

Table 2. Optimization screens of p-TsA

Entry	Solvent	Temperature (°C)	Yield (%)	dr
1	DCM	r.t.	51	1:4
2	Bromobenzene	r.t.	46	1:1
3	THF	r.t.	20	N.R.
4	Toluene	r.t.	63	1:2
6	DCE	0	N.R.	N.R.
7	DCE	-78	N.R.	N.R.
8	DCE	r.t. to 40	38	1:3
9	DCE	r.t. to 80	12	N.R.

While dichloromethane (DCM, entry 1, Table 2) maintained the diastereoselectivity of p-TsA, it did result in lower yields than dichloroethane. The other solvents also were not as favorable as they had both lower yields and either no reaction or lower dr (entries 2-4, Table 2). With DCE determined as the best solvent, the reaction temperature was varied, and we saw similar favorability to the original reaction conditions. Lowering temperature conditions (entries 6 and 7, Table 2) resulted in no reaction. In fact, the -78°C conditions caused DCE to freeze, which was later determined to be due to the melting point of DCE being -35°C. Heating the reactions also did not improve the reaction as raising the temperature to 40°C caused both a decrease in the dr and yield, while heating to 80°C seemed to degrade the starting material completely (entries 8 and

9, Table 2). With the optimum reaction conditions for p-TsA determined, a chiral Brønsted acid catalyst (*S*-TRIP) was used to perform an enantioenriched cyclization.

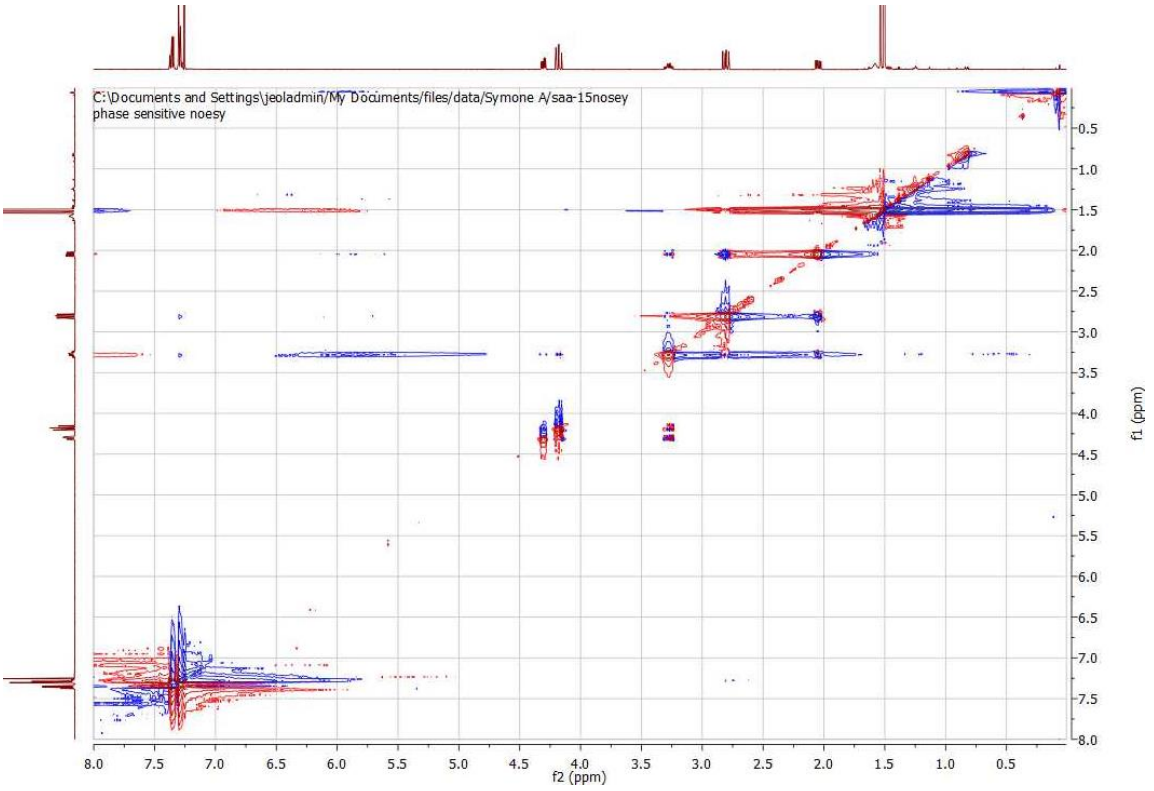

Figure 21. NOESY of isolated major diastereomer for cyclization of **3** with p-TsA

Structural details for compound **3** will be further characterized by X-ray crystallography, but an initial hypothesis is made by Nuclear Overhauser Effect Spectroscopy (NOESY). This method of nuclear magnetic resonance (NMR) spectroscopy provides insight about the spatial interactions of the protons in a compound relative to each other. For compound **3** the main interaction we are interested in exploring is that of proton E on the secondary stereocenter and the protons on the methyl group attached to the α carbon of the lactone ring. As no such interaction is seen in the NOESY of the isolated major diastereomer (Figure 21) it can be assumed that the relative configuration of the

stereocenters of the δ-lactone would have the methyl at the α carbon located in position that would allow for little interaction with proton E. Thus, we predicted that the major diastereomer is the one shown in Figure 22A because its methyl group is in an equatorial location and would not interact through space with proton E.

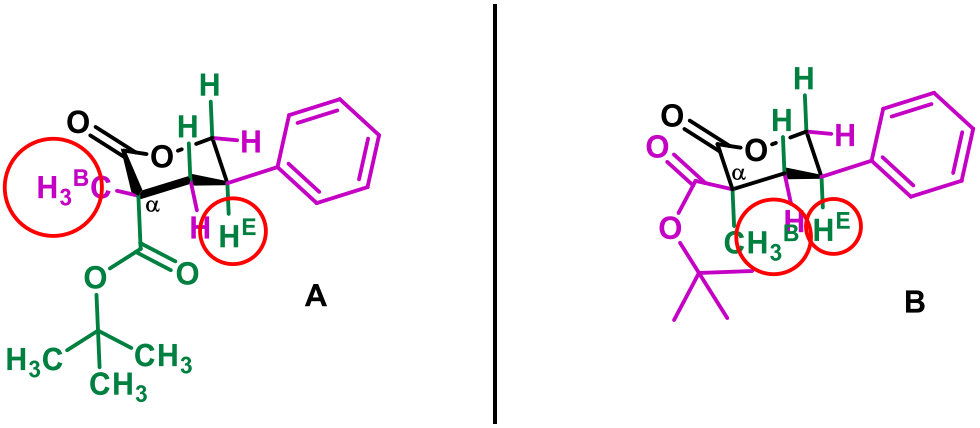

Figure 22. Potential conformations of compound **3**

In an effort to produce enantioenriched diastereomers, TRIP catalyst was used to cyclize compound **2** (Figure 23). Initially *S*-TRIP was used with the optimum conditions found for p-TsA, but this resulted only in recovered starting material. The cyclization was performed twice more, by altering the TRIP catalyst as well as utilizing the reaction conditions similar to those for the coumarin derivatives[18] (Table 3 entries 2 and 3). As seen for Entry 3 in Table 3, the changed from *S*- to *R*- TRIP still resulted in no reaction when performed with DCE as a solvent. Though the reaction with p-TsA in the optimization screen with bromobenzene did not have a high diastereoselectivity, there was a slight increase to dr when the reaction conditions were changed to those used in the coumarin derivative synthesis. The enantioenrichment of each diastereomer proved to be low to moderate with 15% ee for the major isolated diastereomer and 46% ee for

the minor isolated diastereomer. It can also be noted that the major and minor diastereomers were opposite the diastereomers isolated in the cyclization with p-TsA.

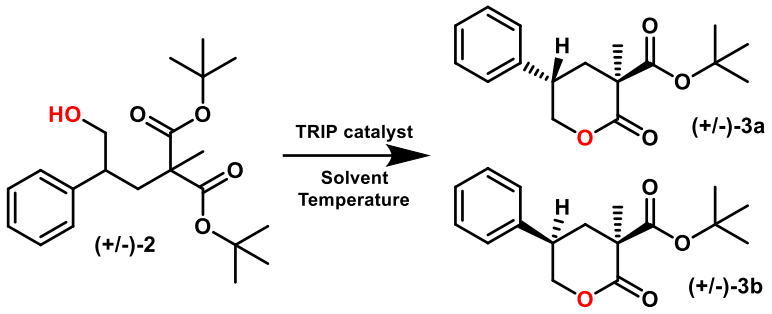

Figure 23. TRIP cyclization for compound **2**

Table 3. TRIP cyclization optimization

Entry	TRIP Catalyst	Temperature	Solvent	Yield (%)	dr	ee_{major}	ee_{minor}
1	*S*	rt to 40°C	DCE	N.R	N.R	N.R	N.R
2	*S*	100°C	Bromobenzene	57	2:1	15%	46%
3	*R*	80°C	DCE	N.R	N.R	N.R	N.R

Based on studies of reactions employing BINOL phosphoric acids, it was determined that there exists a correlation between the acidity of phosphoric acids and their reactivity provided that no catalytic inhibition takes place.[20] Thus it is likely that TRIP catalyst, having a pKa value in the range of 12-14 compared to 8.5 value for p-TsA, was not able to cyclize compound **2** in the optimized reaction conditions because the acidity was not low enough to activate the nucleophilic attack of the hydroxyl group at temperatures at or below 80°C. The difference in the molar equivalence of the catalyst used for cyclization could also factor into the difficulties in the TRIP cyclization as one equivalent of p-TsA was used in the optimization reactions while only 0.05-0.10 equivalents of TRIP were used to cyclize the product.

The preparation of compound **18** (Figure 23) was proposed to compare the diastereoselectivity of the achiral Brønsted acid catalysts. As the secondary stereocenter on this compound was a methyl and not a phenyl ring, it would be likely that the enantioselectivity of this compound would decrease as the pi stacking from the phenyl group that was theorized previously by the Petersen group to aid in the selectivity of the cyclization was no longer present.[18] Unfortunately, due to issues with TLC visualization as well as poor reaction yields, compound **17** was unable to be fully characterized for further synthesis.

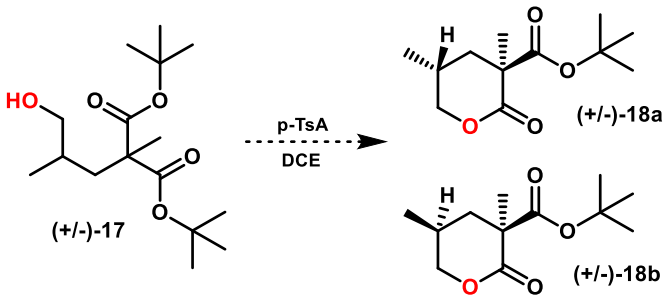

Figure 24. Cyclization of compound **17**

II.2 Future Work and Conclusions

While this work was able to achieve novel diastereoselectivity with Brønsted acid catalyzed cyclizations, further optimization and study of these results will likely need to be continued to promote even greater selectivity. Additionally, while the NOESY was able to assist in theorizing the conformation of the isolated major diastereomer of the cyclization with p-TsA, X-ray crystallography will be necessary to confirm the predicted relative stereochemistry of this diastereomer. Though it was not specified in the previous section the results from the reaction monitoring of Entry 2 of Table 3 indicate that longer reaction time might be necessary potentially leading to an increase of the dr or reaction

yield. This is likely as some starting material was still present when the reaction was stopped after a 24-hour reaction period. Additionally employing *R*-TRIP in conditions detailed in Entry 2 may reveal if the configuration of the catalyst might factor into the diastereo- and enantioselectivity of this cyclization. Based on the concept of matched/mismatched effects, it could be likely that the low diastereoselectivity seen for *S*-TRIP was due to a mismatched paring of the catalyst and the starting material and that utilizing *R*-TRIP would lead to an increase of diastereoselectivity based on a potentially more matched pairing where the multiple stereocenters would be situated in a more favorable conformation for stereocontrolled interactions.[21] The main prediction being that the free energy differences would be greater for the matched than the mismatched catalyst and substrate pair.[22] Next, further screening of both solvent systems and other BINOL phosphoric acid catalysts may provide increased selectivity as alterations of each reaction component may lower the activation necessary to promote cyclization. Finally, expanding not only the substrate scope of the secondary alkylating agent but also determining a successful process for synthesizing compound **17** would help to validate the robustness of these novel Brønsted acid catalyzed cyclizations for both diastereo- and enantioselectivity.

CHAPTER III

EXPERIMENTAL PROCEDURES AND RESULTS

III.1 General Information

Solvents and reagents were obtained from commercial sources and did not undergo purification unless stated. The ^{1}H and ^{13}C nuclear magnetic resonance (NMR) spectra were conducted on the 400 and 500 MHz spectrometer at room temperature with chloroform-D ($CDCl_3$) as the solvent. The NMR chemical shifts (δ) are reported in ppm. Abbreviations for ^{1}H NMR: s=singlet, d=doublet, m=multiplet, t=triplet, q=quartet. The reactions were monitored by TLC using silica gel (particle size: 40-63 μm, 230x400 mesh) and GC/FID analysis. Enantiomeric excess was determined by HPLC analysis. High Resolution Mass Spectra were acquired at UNCG Triad Mass Spectrometry Laboratory.

III.2 Synthesis of Compound **3**

III.2.1 Synthesis of Monobrominated Alkylating agent **9**

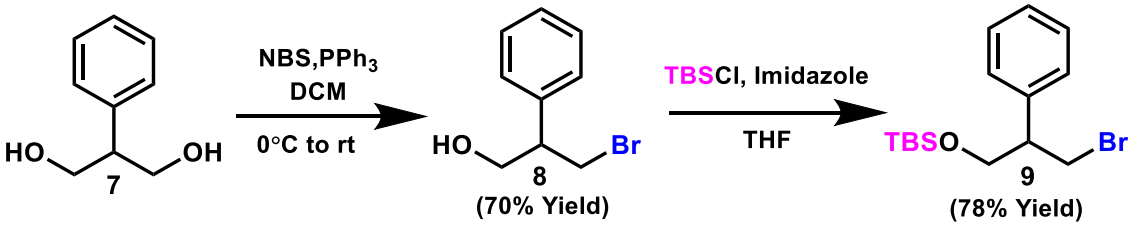

Figure 25. Monobromination and protection to synthesize alkylating agent **9**

To begin *N*-bromosuccinimide (NBS; 5.69 g, 33.5 mmol) was added at 0 °C to a mixture of **7** (5.00 g, 32.9 mmol) and triphenylphosphine (PPh_3; 8.59 g, 32.8 mmol) dissolved in dry dichloromethane (DCM; 140 mL) in a 250 mL flame dried two neck round bottom flask under argon. The cooling bath was removed, and the reaction allowed to warm to room temperature and stirred for five days. The solvent was then evaporated, and the product was purified by column chromatography (Silica gel, 1:5 ethyl acetate: hexane), to yield compound **8** as a clear yellowish liquid (4.91 g, 70% yield) which was used directly in the next step. ^{1}H NMR (400 MHz, $CDCl_3$) δ 7.40-7.25 (m, 4H), 7.23 (s, 1H), 3.96 (d, *J*= 5.9 Hz, 2H), 3.81-3.68 (m, 1H), 3.64 (m, *J*= 10.1, 6.5 Hz, 1H), 3.20 (m, *J*= 6.3 Hz, 1H) ppm

A mixture of compound **8** (1.00 g, 18 mmol) in tetrahydrofuran (THF; 10mL) was reacted with imidazole (950 mg, 54 mmol) and tert-butyldimethylsilylchloride (TBS-Cl; 1.19 g, 31 mmol) in anhydrous THF (50 mL) was stirred in a 100 mL flame dried two neck round bottom flask under argon at room temperature overnight. The mixture was diluted with water (40 mL) and extracted three times with DCM (50 mL each). The organic layers were combined and dried over magnesium sulfate ($MgSO_4$), which was then filtered off. The mixture was then concentrated and purified by column chromatography (Silica gel, 1:8 ethyl acetate: hexane) to obtain substituted (3-bromopropoxy)-*tert*-butyldimethylsilanes, **9** as a clear liquid (1.53 g, 78% yield). ^{1}H NMR (400 MHz, $CDCl_3$) δ 7.34-7.26 (m, 2H), 7.26-7.20 (m, 3H), 3.94-3.77 (m, 3H), 3.63 (m, *J*= 9.9, 7.1 Hz, 1H), 3.12 (m, *J*= 6.5, 4.4 Hz, 1H), 0.87 (s, 9H), -0.00 (d, *J*= 4.0 Hz 6H) ppm; ^{13}C NMR (400 MHz, $CDCl_3$) δ 140.5, 128.5, 128.1, 127.3, 65.1, 50.2, 34.9, 25.9, 18.3, -5.4 ppm; HRMS (ESI): for $C_{15}H_{25}BrOSi$ $[M+H]^+$: calculated 329.0931; found 329.0923

III.2.3 Total Alkylation of **2** with Compound **9** and Iodomethane

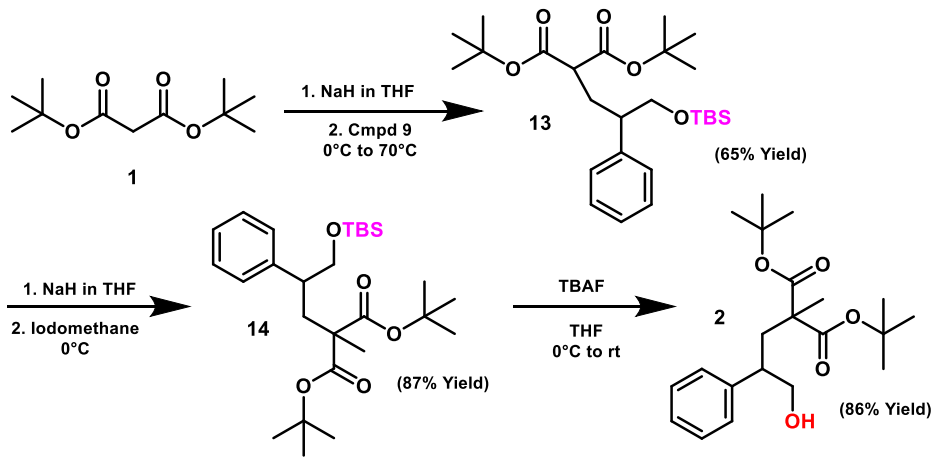

Figure 26. Alkylation of compound **1** with compound **9** and iodomethane followed by deprotection

For the first alkylation, sodium hydride (NaH; 314 mg, 7.9 mmol) in THF (80 mL) was cooled to 0 °C in a 100 mL flame dried two neck round bottom flask under argon in an ice bath then the di-*tert*-butyl malonate **1** (1.62 mL, 7.2 mmol) was added followed by the alkylating agent **9** (1.18 g, 3.6 mmol) and the reaction was allowed to warm slightly to room temperature before placing the flask in an oil bath which was heated to ~65 °C. The reaction was stirred overnight before being dilute with water (50 mL) and extracted 3 times with DCM (100 mL each). The organic layers were combined and dried over $MgSO_4$, then filtered and concentrated. Compound **13** was isolated by column chromatography (Silica gel, 1:12.5 ethyl acetate: hexane), to yield a clear liquid (1.08 g, 65% yield). In the second alkylation, NaH (492 mg, 12.3 mmol) in THF (60 mL) was again cooled to 0 °C in a 100 mL flame dried two neck round bottom flask under argon in an ice bath then the substituted malonate **13** (2.34 g, 5.0 mmol) was added followed by iodomethane (674 μL, 10.8 mmol). The flask was warmed to room temperature and the reaction stirred overnight, before being dilute with water (50 mL) and extracted with three times with DCM (100mL each).

The organic layers were combined and dried over $MgSO_4$ then filtered and concentrated, followed by purification by column chromatography (Silica gel, 1:50 ethyl acetate: hexane) for a clear liquid of the fully alkylated product **14** (1.73 g, 87% yield). The tert-butyldimethylsilane protecting group was then removed by dissolving **14** (1.32 g, 2.8 mmol) in THF (30 mL) in a 100 mL flame dried two neck round bottom flask under argon in an ice bath at 0 °C. Tetra-n-butylammonium fluoride (TBAF; 1.26 mL, 4.8 mmol) was added dropwise while stirring. The flask was stirred overnight to reach room temperature. The reaction was then quenched with water (30 mL) and extracted three times with DCM (30 mL each). The organic layers were combined and dried over $MgSO_4$, then filtered and concentrated. Compound **2** was then isolated by column chromatography (Silica gel, 1:14.3 ethyl acetate: hexane) as a clear liquid (861 mg, 86% yield). ^{1}H NMR (400 MHz, $CDCl_3$) δ 7.28 (d, *J*= 7.9 Hz, 2H), 7.21 (m, 3H), 3.69-3.57 (m, 2H), 2.80 (s, 1H), 2.32 (d, *J*= 12.8 Hz, 1H), 2.17-2.09 (m, 1H), 1.44 (s, 9H), 1.32 (s, 9H), 1.18 (s,3H) ppm; ^{13}C NMR (400 MHz, $CDCl_3$) δ 143.0, 128.8, 128.4, 127.0, 81.5, 81.4, 68.2, 54.78, 44.8, 37.0, 27.9, 27.8, 20.5 ppm; HRMS (ESI): for $C_{21}H_{32}O_5$ $[M+H]^+$: calculated 365.2323; found 365.2314

III.2.4 Cyclization of **2**

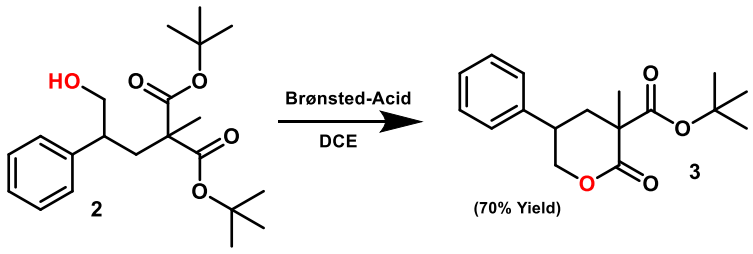

Figure 27. Cyclization of compound **2**

In a flame dried 50 mL round bottom flask, compound **2** (300 mg, 0.82 mmol) was dissolved in DCE (15 mL) before the Brønsted acid catalyst (1 equivalent, Table 1) was

added. The reaction was stirred overnight, before being dilute with water (15mL) and extracted three times with ethyl acetate (20 mL each). The organic layers were combined and dried over $MgSO_4$, then filtered and concentrated. Compound **3** was then isolated by column chromatography (Silica gel, 1:20 to 1:6 ethyl acetate: hexane) and concentrated to white crystals (168 mg, 70% yield). ^{1}H NMR (400 MHz, $CDCl_3$) δ 7.38-7.32 (m, 2H), 7.29 (d, *J*= 12.8 Hz, 3H), 4.30 (m, *J*= 11.1, 5.0, 1.8 Hz, 1H), 4.17 (t, *J*= 11.8 Hz, 1H), 3.27 (m, *J*= 12.3, 10.1, 7.6, 4.9 Hz, 1H) 2.80 (m, *J*= 14.1, 10.1 Hz, 1H), 2.04 (m, *J*= 14.2, 7.4, 1.8 Hz, 1H), 1.53 (s, 3H), 1.50 (s, 9H) ppm; ^{13}C NMR (400 MHz, $CDCl_3$) δ 171.2, 167.9, 139.0, 129.1, 127.8, 127.7, 83.0, 72.7, 50.9, 39.0, 37.6, 27.8, 23.5 ppm; HRMS (ESI): for $C_{17}H_{22}O_4$ $[M+H]^+$: calculated 291.15; found 291.16

III.3 Synthesis of Compound **17**

III.3.1 Synthesis of Compound **15**

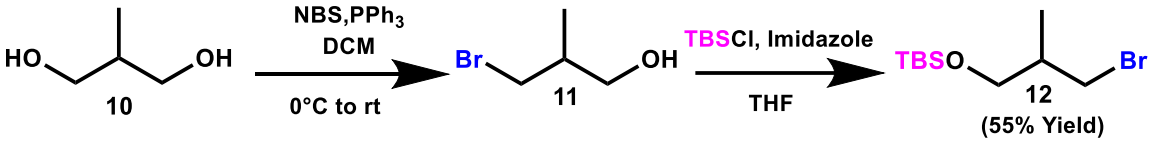

Figure 28. Monobromination and protection to synthesize alkylating agent **12**

NBS (6.26 g, 35.2 mmol) was added at 0 °C to a mixture of **10** (2.5 mL, 28.2 mmol) and PPh_3 (9.23 g, 35.2 mmol) dissolved in dry DCE (200 mL) in a 250 mL flame dried two-neck round bottom flask under argon. The cooling bath was removed, and the flask allowed to warm to room temperature and stirred for three days. The solvent was then quenched with water (100 mL) and extracted three times with DCM (75 mL each). The organic layers were combined and dried over $MgSO_4$, then filtered. The product was then concentrated to yield compound **11** as a yellowish crystal. Due to visualization

issues compound **11** could not be purified by column chromatography, so it was used directly in the next step. Compound **11** (4.31 g, 20.0 mmol) was then placed in a 250 mL two-necked round bottom flask and reacted with imidazole (3.70 g, 40.1 mmol) and TBS-Cl (5.13 g, 34.1 mmol) in anhydrous THF (50 mL) stirred at room temperature overnight. The mixture was diluted water (100 mL) and extracted three times with DCM (50 mL each). The organic layers were combined and dried with $MgSO_4$ then filtered. The solvent was evaporated to obtain substituted (3-bromopropoxy)-*tert*-butyldimethylsilane, **12**, as a yellow liquid (2.95 g, 55% yield). Again due to visualization issues compound **12** could not be purified by column chromatography, so it was used directly in the next step.

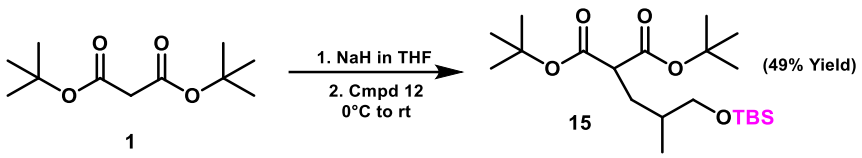

Figure 29. Alkylation of compound **1** with compound **12**

To a flame dried two-neck 100 mL round bottom flask, NaH (782 mg, 19.5 mmol) in THF (50 mL) was cooled to 0 °C in an ice bath then the di-*tert*-butyl malonate **1** (2.99 mL, 13.2 mmol) was added followed by the alkylating agent **12** (2.95 g, 11.0 mmol) and the reaction was allowed to warm slightly to room temperature. The reaction was stirred for three days before being dilute with water (50 mL) and extracted three times with DCM (25 mL each). The organic layers were combined and dried over $MgSO_4$, then filtered. The solvent was evaporated and compound **15** was isolated by column chromatography (Silica gel, 15% ethyl acetate: hexane) and concentrated to a yellow liquid (2.17 g, 49% yield). ^{1}H NMR (400 MHz, $CDCl_3$) δ 4.08 (t, *J*= 6.7 Hz ,3H), 3.56-3.49 (m, 1H), 3.48-3.35 (m, 2H), 1.45 (s, 9H), 1.43 (s, 9H), 0.87 (s, 9H), 0.01 (s, 6H) ppm; ^{13}C NMR (400 MHz,

$CDCl_3$) δ 167.2, 82.1, 67.0, 44.5, 28.3, 26.0, 22.0, 10.4, -5.3 ppm; HRMS (ESI): for $C_{21}H_{42}O_5Si$ $[M+H]^+$: calculated 403.2874; found 403.2868

III.3.2 Second Alkylation of Compound **15** and Deprotection

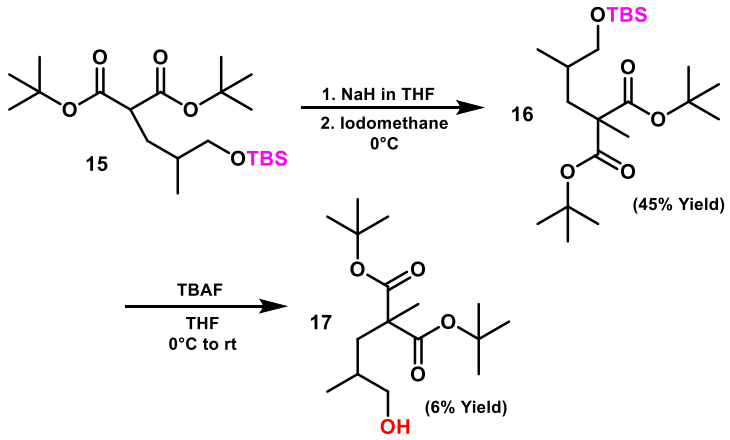

Figure 30. Alkylation of Compound **15** with iodomethane followed by deprotection

In the second alkylation, NaH (406 mg, 10.2 mmol) in THF (50 mL) was cooled to 0 °C in a 100 mL flame dried two neck round bottom flask under argon in an ice bath then the substituted malonate **15** (1.95 g, 5.0 mmol) was added followed by iodomethane (674 μL, 10.8 mmol). The flask was warmed to room temperature and stirred overnight, before being dilute with water (50 mL) and extracted three times with DCM (20 mL each). The organic layers were combined and dried over $MgSO_4$, then filtered. The solvent was evaporated and purified by column chromatography (Silica gel, 5% ethyl acetate in hexane) for a fully alkylated product **16**. The product was concentrated to a light orange colored liquid (908 mg, 45%yield). The tert-butyldimethylsilane protecting group was then removed by dissolving **16** (908 mg, 2.2 mmol) in THF (20 mL) in a 100 mL flame dried two neck round bottom flask under argon, then cooling it to 0 °C in an ice bath. TBAF (3.27 mL, 3.27 mmol) was added dropwise while stirring. The reaction was stirred overnight to

reach room temperature. The reaction was then quenched with water (20 mL) and extracted three times with DCM (15 mL each). The organic layers were combined and dried over $MgSO_4$, then filtered Compound **17** was then isolated by column chromatography (Silica gel, 7% ethyl acetate in hexane). The product was concentrated to a light-yellow liquid (40 mg, 6%yield). Peaks from spectra do not correlate with what would be expected for this compound.

REFERENCES

1) Nguyen, L. A.; He, H.; Pham-Huy, C. *Int. J. Biomed. Sci.* **2006**, *2*, 85-100.
2) Muñoz Solano, D.; Hoyos, P.; Hernáiz, M.J.; Alcántara, A.R.; Sánchez-Montero, J.M. *Bioresour. Technol*. **2012,** *115*, 196–207.
3) Wilent, J. E.; Petersen, K. S. *J. Org. Chem*. **2014**, *79*, 2303-2307.
4) Akiyama, T. *Chemical Reviews.* **2007**, *107* (12), 5744–5758.
5) Li, P.; Hu, X.; Dong, X.-Q.; Zhang, X. *Molecules.* **2016**, *21* (10), 1327.
6) Brown, J. M.; Conn, A. D.; Pilcher, G.; Leitão, M. L. P.; Meng-Yan, Y. *J. Chem. Soc., Chem. Commun.* **1989**, *23*, 1817–1819.
7) Li, H.; Shakaroun, R. M.; Guillaume, S. M.; Carpentier, J. F. *Chemistry – A European Journal.* **2019**, *26* (1), 128–138.
8) Yang, J., Jia, L., Yin, L., Yu, J., Shi, Z. Fang, Q., Cao, A. *Macromol. Biosci.* **2004**, *4*, 1092
9) Jung, M. E.; Piizzi, G. *Chemical Reviews.* **2005**, *105* (5), 1735–1766.
10) Changotra, A.; Sunoj, R. B. *Org. Lett.* **2016**, *18* (15), 3730–3733.
11) Qabaja, G.; Benavides, A. R.; Liu, S.; Petersen, K. S. *J. Org. Chem.* **2014**, *80* (1), 133–140.
12) Li, X.; Li, H.; Zhao, Y.; Tang, X.; Ma, S.; Gong, B.; and Li, M. *Polym. Chem*. **2015**, *6*, 6452–6456
13) Kim, H.; Olsson, J. V.; Hedrick, J. L.; and Waymouth, R. M. *ACS Macro Lett.* **2012**, *1*, 845.
14) Johnson, R.; Riggs, N.V. *Tetrahedron Letters,* **1967**, *8* (50), 5119–5122.

15) Keith, J. M.; Larrow, J. F.; Jacobsen, E. N. *Advanced Synthesis & Catalysis,* **2001**, *343* (1), 5–26.

16) Shakaroun, R. M.; Slawinski, M.; Carpentier, J.-F.; Guillaume, S. M. *European Polymer Journal,* **2020**, *134*, 109858.

17) Terada, M. *Synthesis.* **2010**, *2010* (12), 1929–1982.

18) Kelley, A. M.; Haywood, R. D.; White, J. C; Petersen, K. S. *Chemistry Select.* **2020**, *5*, 3018-3022

19) Ng, D.; Yang, Z.; Garcia-Garibay, M.A. *Organic Letters.* **2004**, *6* (4), 645-647

20) Parmar, D.; Sugiono, E.; Raja, S.; Rueping, M*. Chem. Rev.* **2014**, *114*, 9047−9153

21) Doyle, M.P.; Morgan, J.P.; Fettinger, J.C.; Zavalij, P.Y.; Colyer, J.T.; Timmons, D.J.; Carducci, M.D*. J. Org. Chem.* **2005**, *70*, 5291-5301

22) Richards, C.J.; Arthurs, R.A. *Chem. Eur. J*. **2017**, *23*, 11460 – 11478

23) Liu, C; Wen, K.G.; Zeng, X.P.; Peng, Y.Y. *Adv*. *Synth. Catal.* **2020**, *362,* 1015-1031

24) Mao, B; Fañanas-Mastral, M.; Feringa, B.L. *Chem. Rev.* **2017**, *117*, 10502−10566

APPENDIX A

NMR SPECTRA

The ^{1}H and ^{13}C nuclear magnetic resonance (NMR) spectra were plotted on 400 MHz spectrometer using $CDCl_3$ as a solvent at room temperature. The NMR chemical shifts (δ) are reported in ppm. Abbreviations for ^{1}H NMR: s = singlet, d = doublet, m = multiplet, b = broad, t = triple, q = quartet.

^{1}H NMR

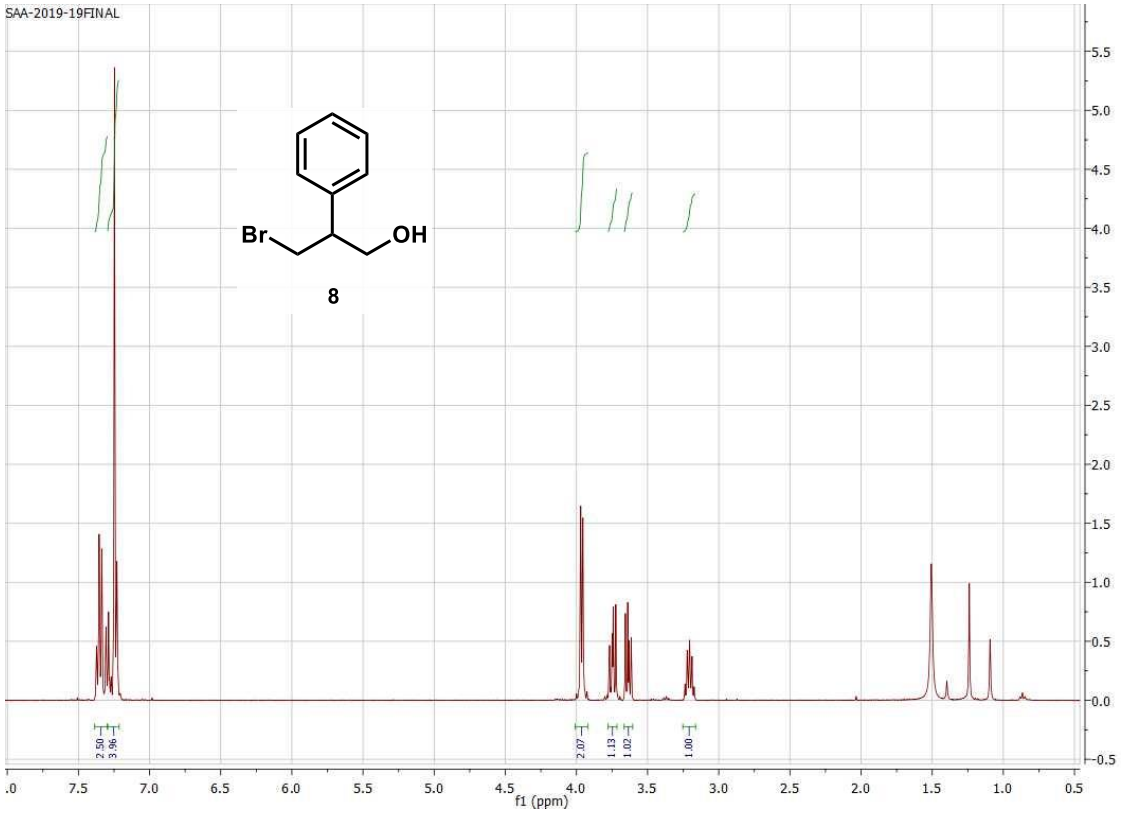

^{1}H NMR

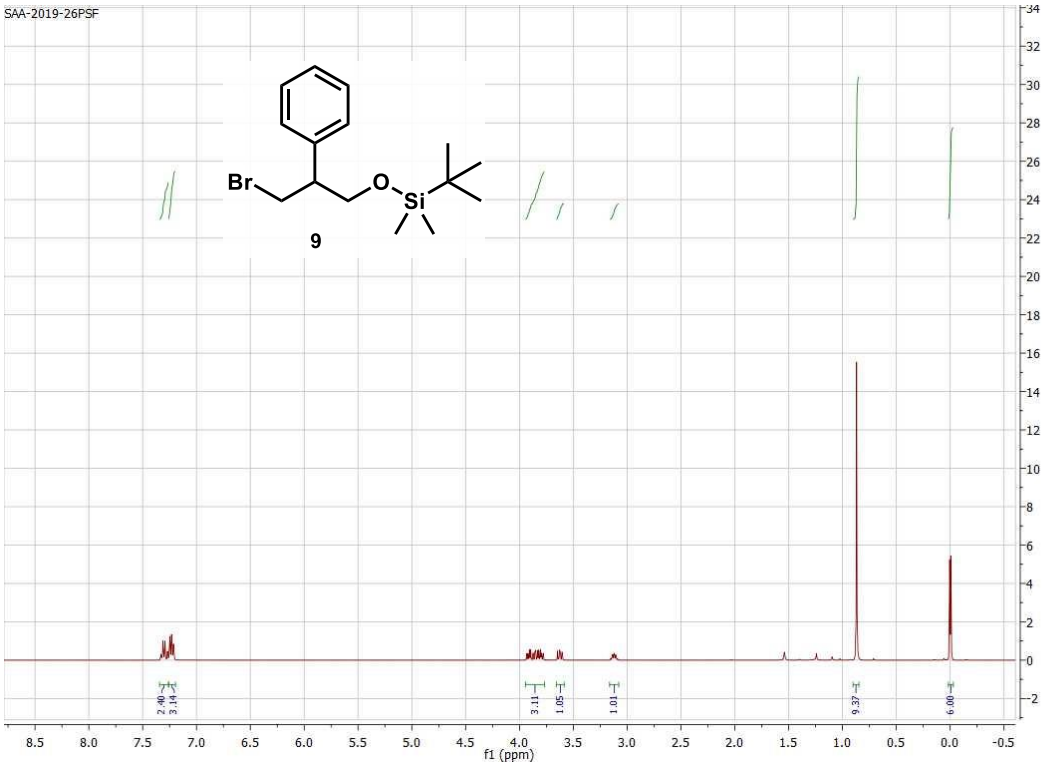

^{13}C NMR

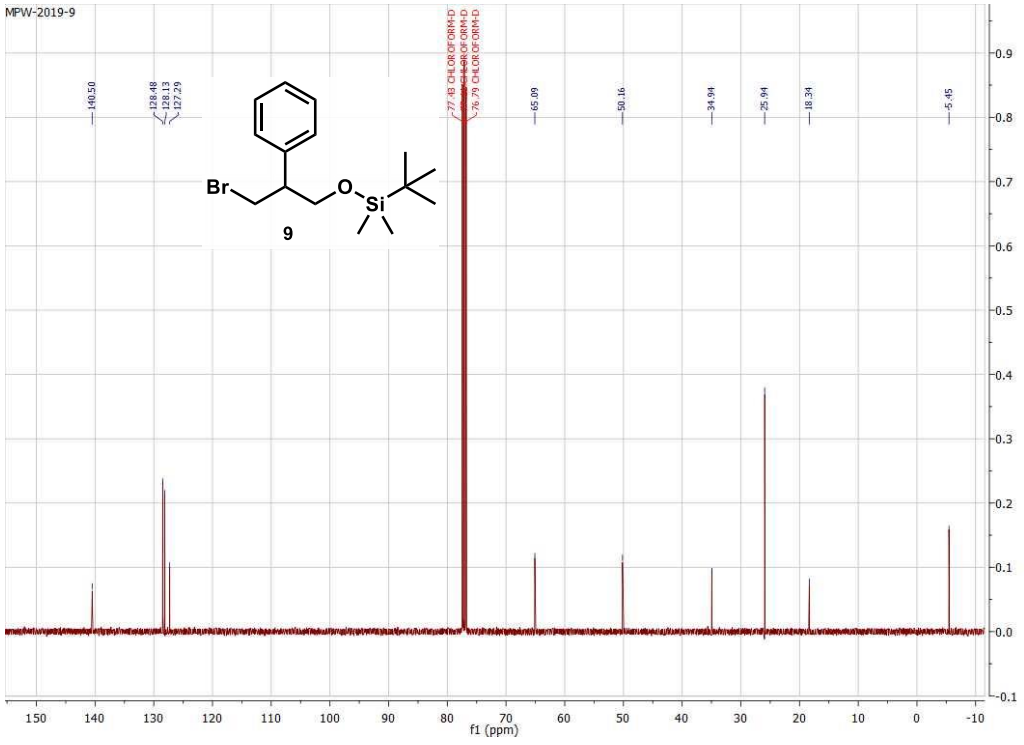

^{1}H NMR

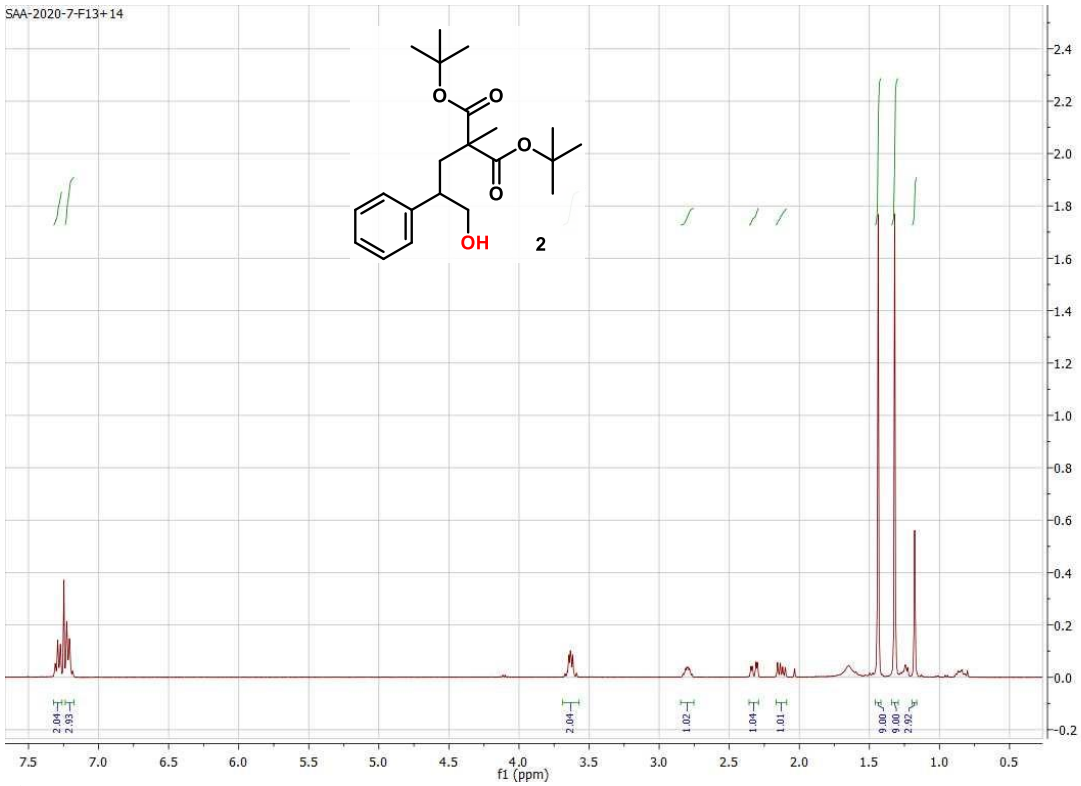

^{13}C NMR

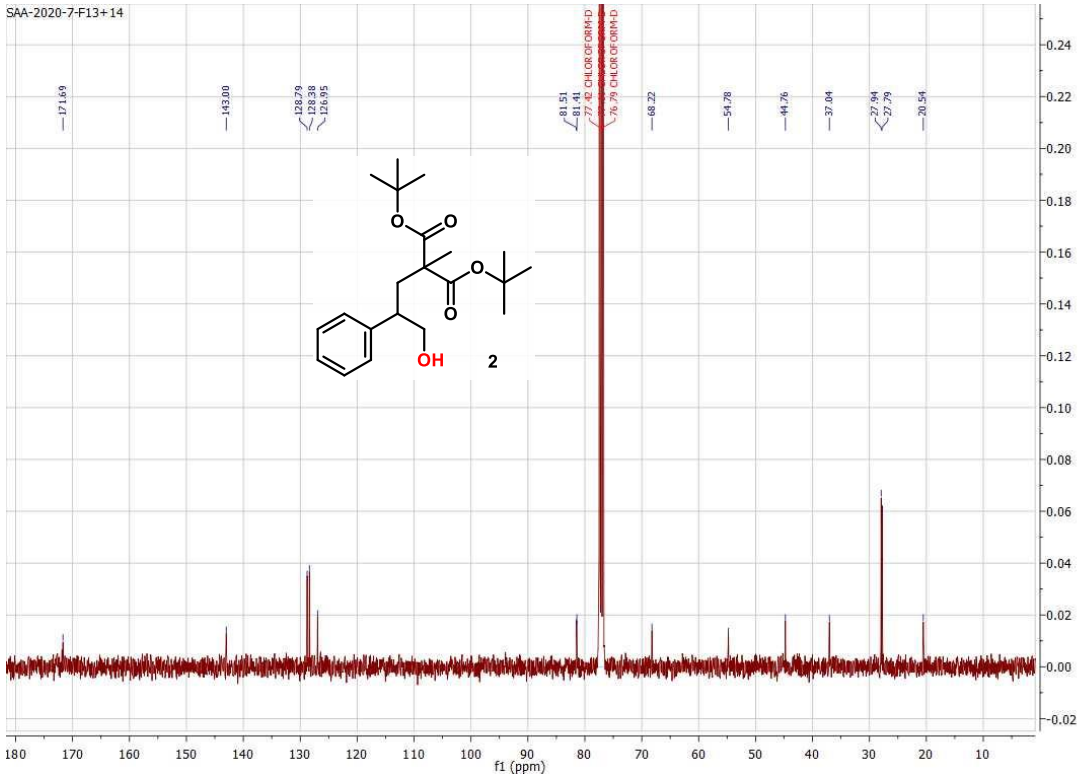

^{1}H NMR

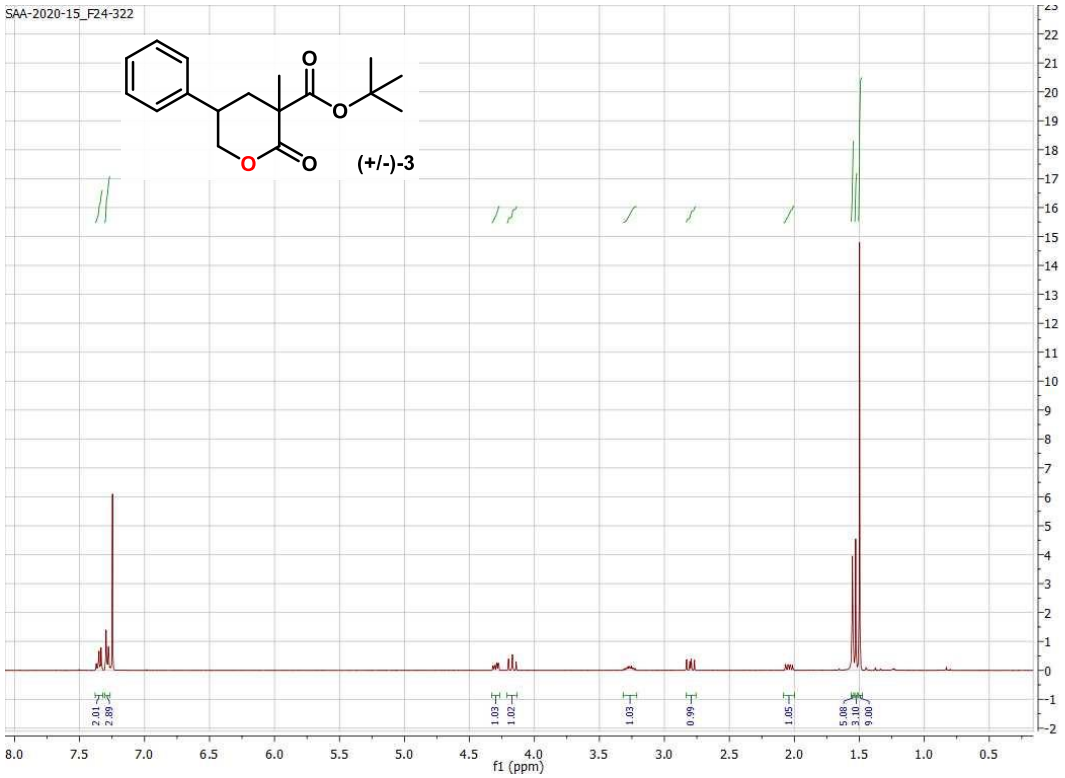

^{13}C NMR

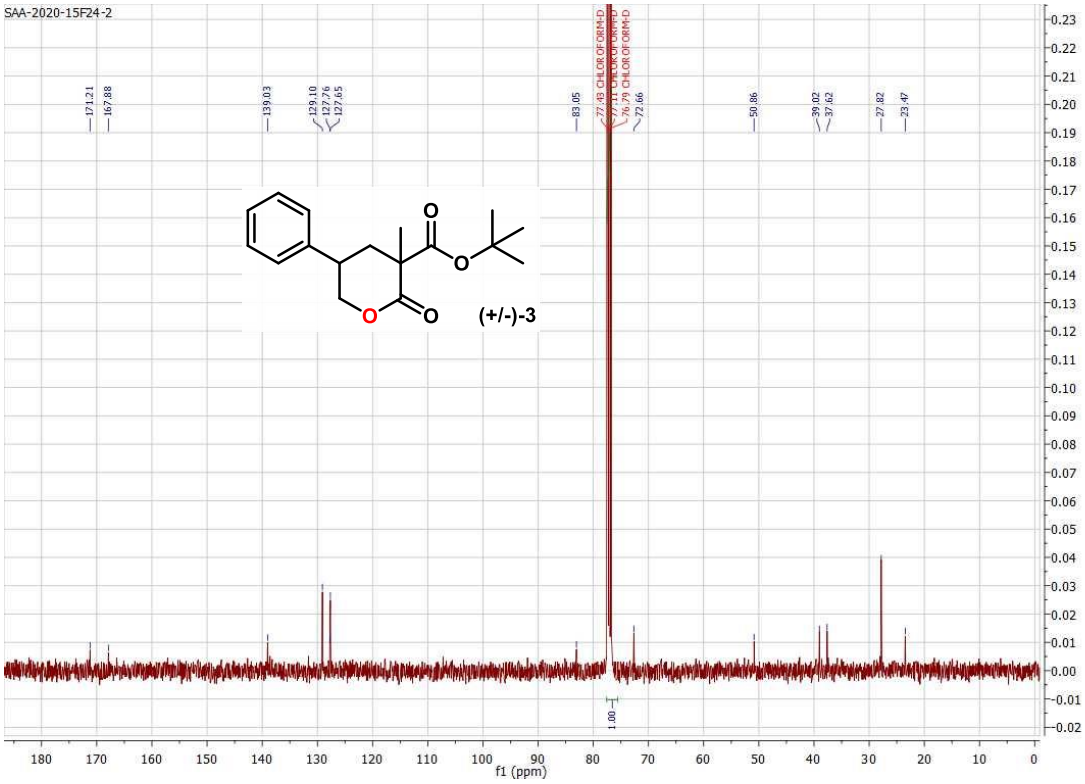

^{1}H NMR

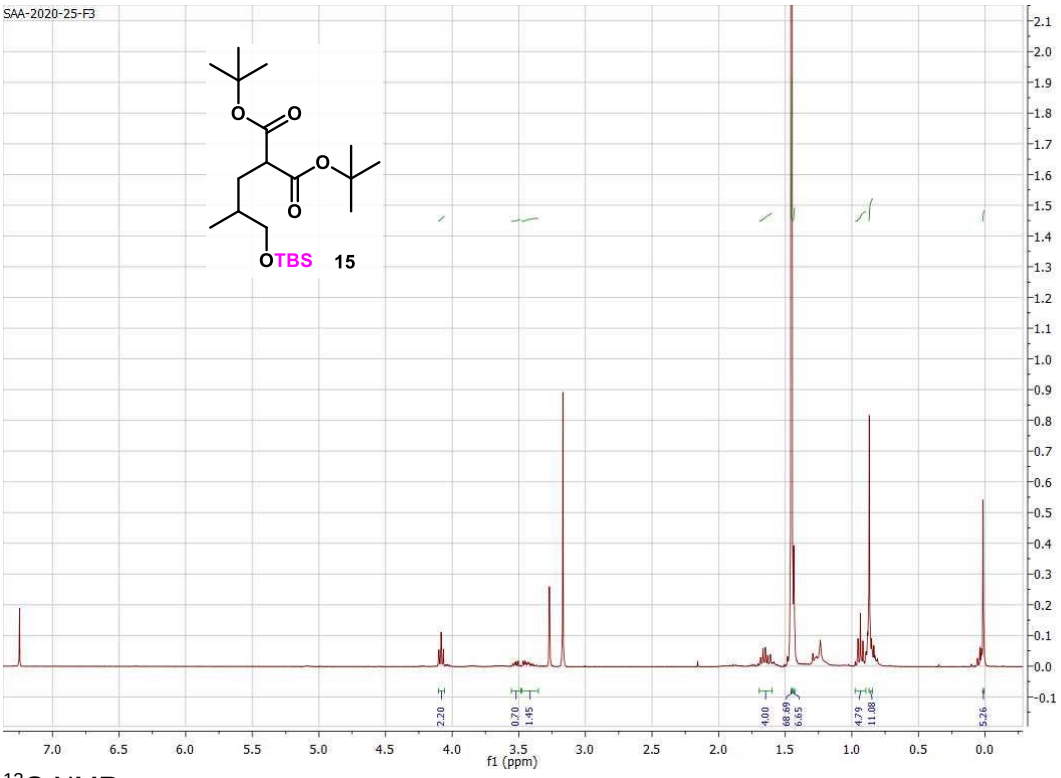

^{13}C NMR

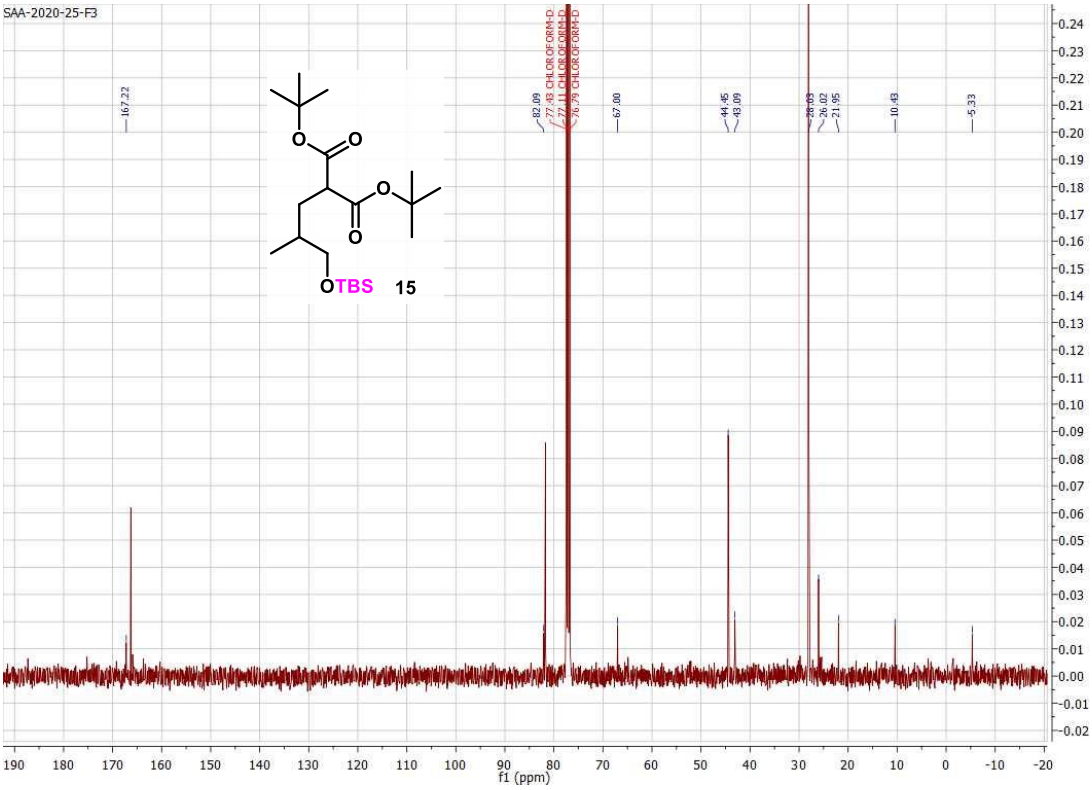

^{1}H NMR

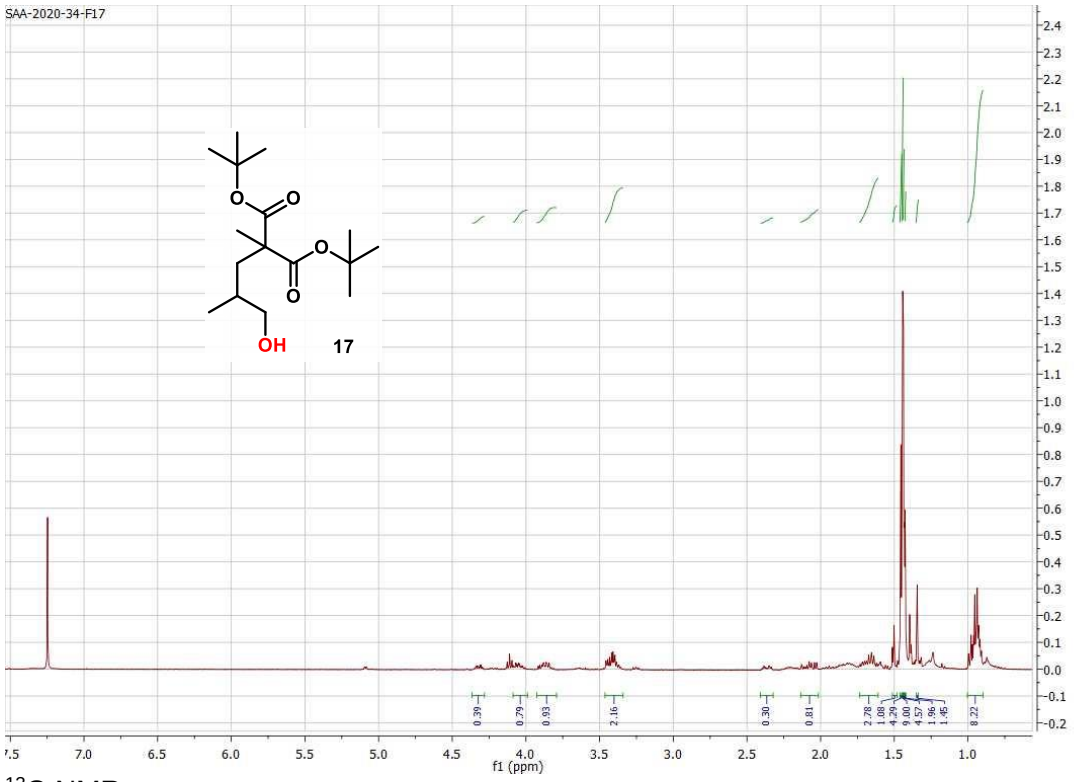

^{13}C NMR

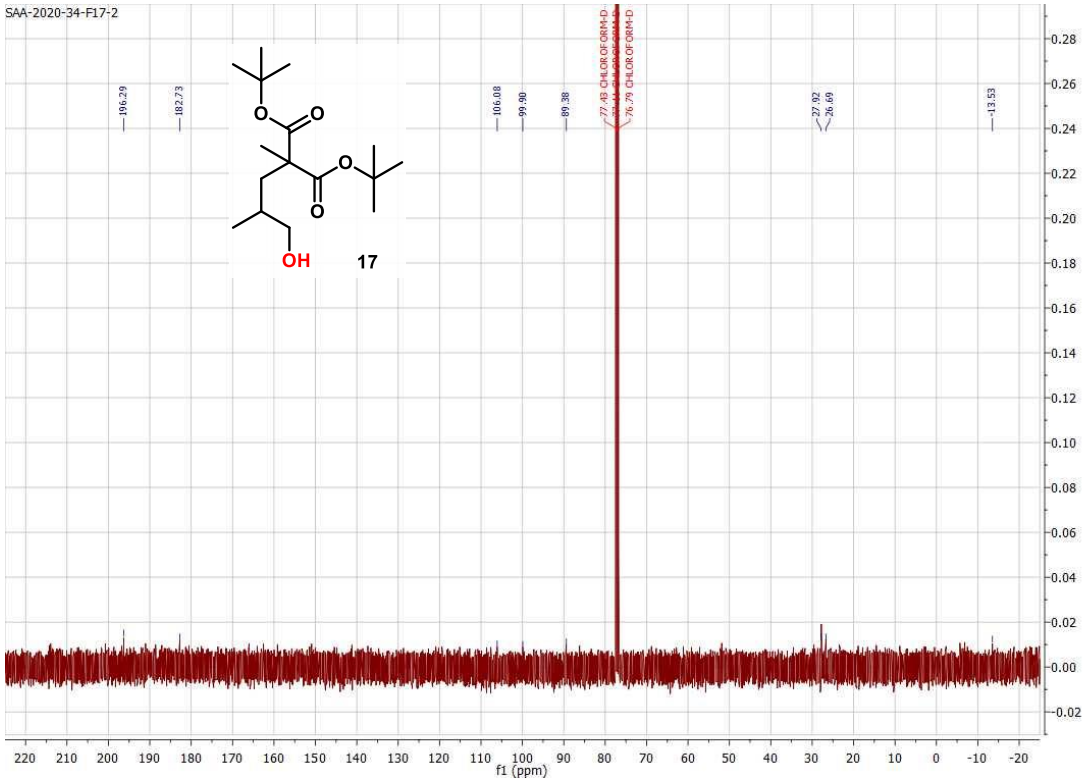

APPENDIX B

CHROMATOGRAMS

HPLC chromatograms were obtained using an Agilent 1260 Infinity with diode array detector (DAD) and a CHRIALCEL AD-H (4.6 mm x 250 mm x 5 μm) chiral column. Analysis details can be found with the chromatogram. High Resolution Mass Spectra were acquired at UNCG Triad Mass Spectrometry Laboratory.

Major Diastereomer of p-TsA cyclization:

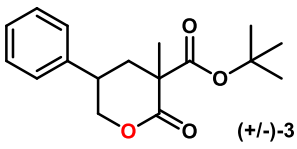

(+/-)-3

HPLC Conditions: Column: HPLC AD-H 4.6 mm x 250 mm x 5 μm; Eluent Rate: 1mL/min; Eluent: 5% IPA/hexane; Monitoring wave: 254 nm

Racemic:
Major product

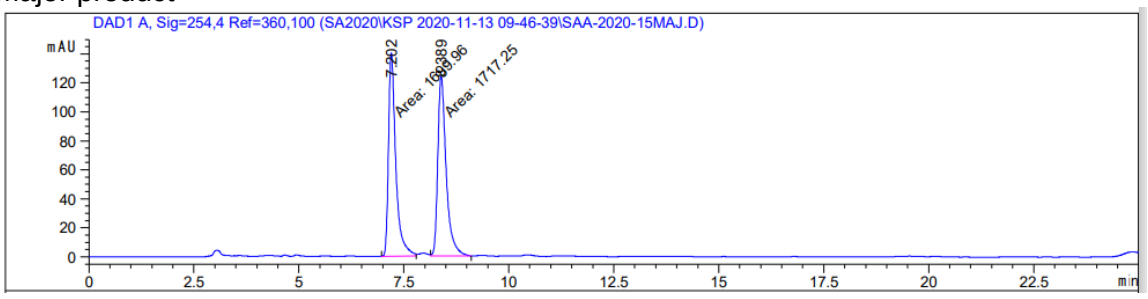

Signal 1: DAD1 A, Sig=254,4 Ref=360,100

Peak #	RetTime [min]	Type	Width [min]	Area [mAU*s]	Height [mAU]	Area %
1	7.202	FM	0.2019	1699.95557	140.35248	49.7469
2	8.389	MF	0.2311	1717.25110	123.84660	50.2531

Minor Product

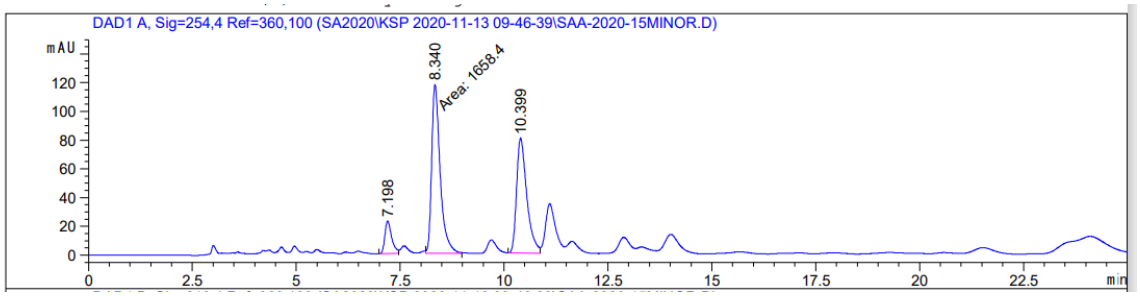

Signal 1: DAD1 A, Sig=254,4 Ref=360,100

Peak #	RetTime [min]	Type	Width [min]	Area [mAU*s]	Height [mAU]	Area %
1	7.198	BV	0.1739	261.97809	22.83419	7.9584
2	8.340	MF	0.2355	1658.40198	117.37497	50.3788
3	10.399	BV	0.2580	1371.48218	79.99265	41.6628

Enantiomeric:

Bromobenzene (Minor Product)

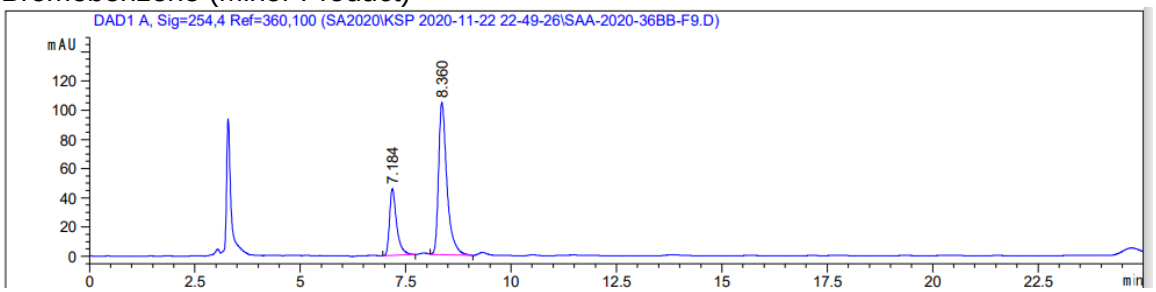

Signal 1: DAD1 A, Sig=254,4 Ref=360,100

Peak #	RetTime [min]	Type	Width [min]	Area [mAU*s]	Height [mAU]	Area %
1	7.184	BB	0.1739	530.11255	45.52118	26.8758
2	8.360	VB	0.2050	1442.34033	104.54518	73.1242

Bromobenzene (Major Product)

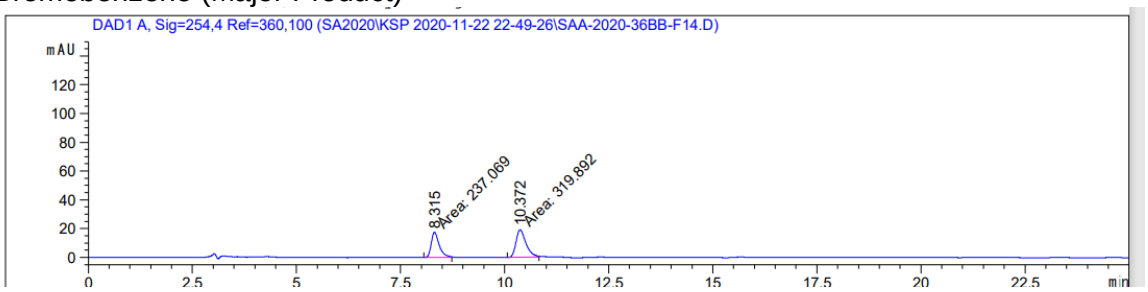

Signal 1: DAD1 A, Sig=254,4 Ref=360,100

Peak #	RetTime [min]	Type	Width [min]	Area [mAU*s]	Height [mAU]	Area %
1	8.315	MF	0.2245	237.06947	17.59608	42.5648
2	10.372	MF	0.2770	319.89243	19.24956	57.4352

MPW-2019-9-1 Mass Peak found

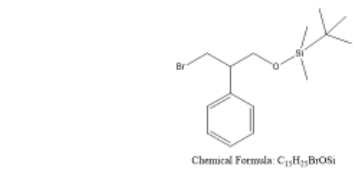

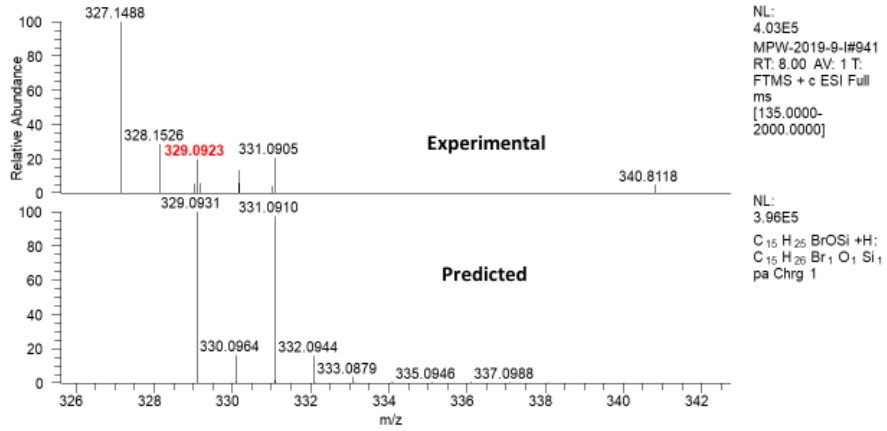

MPW-2019-9-1 Mass Peak found

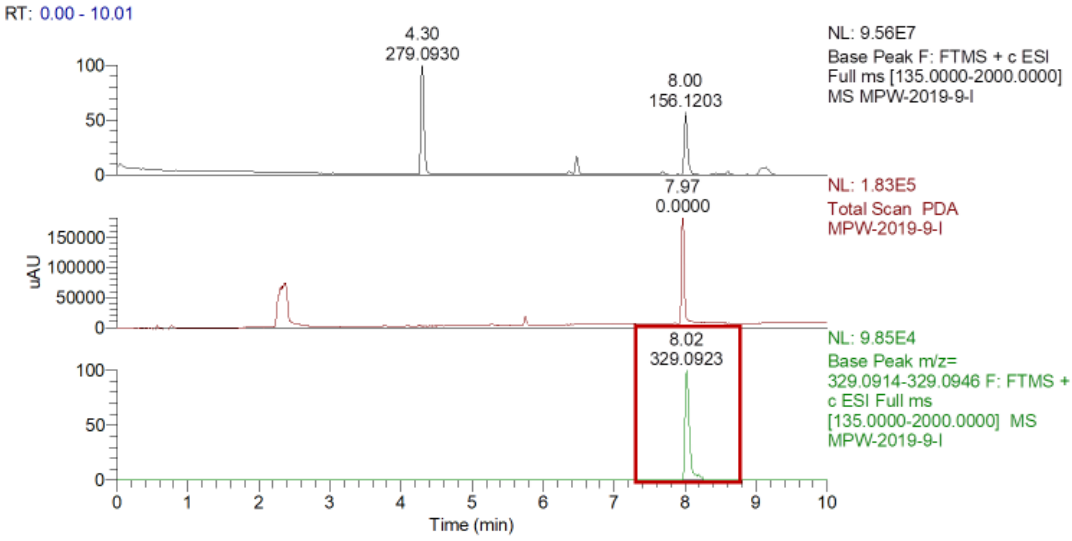

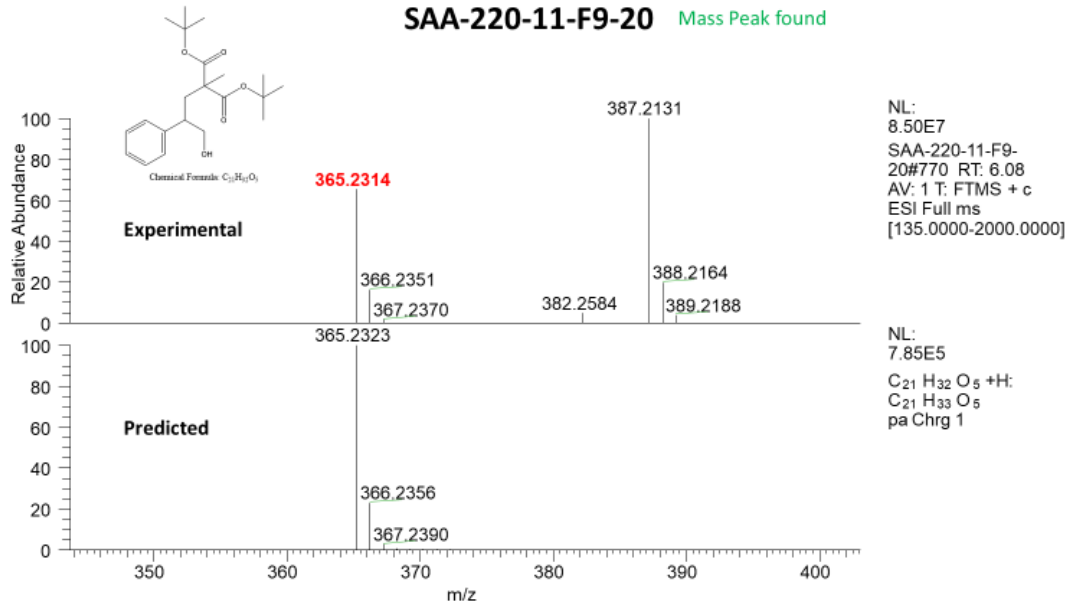
SAA-220-11-F9-20
Mass Peak found
Experimental
Predicted
Relative Abundance
m/z
365.2314
387.2131
366.2351
367.2370
382.2584
388.2164
389.2188
365.2323
366.2356
367.2390
NL:
8.50E7
SAA-220-11-F9-20#770 RT: 6.08 AV: 1 T: FTMS + c ESI Full ms [135.0000-2000.0000]
NL:
7.85E5
C21 H32 O5 +H:
C21 H33 O5
pa Chrg 1

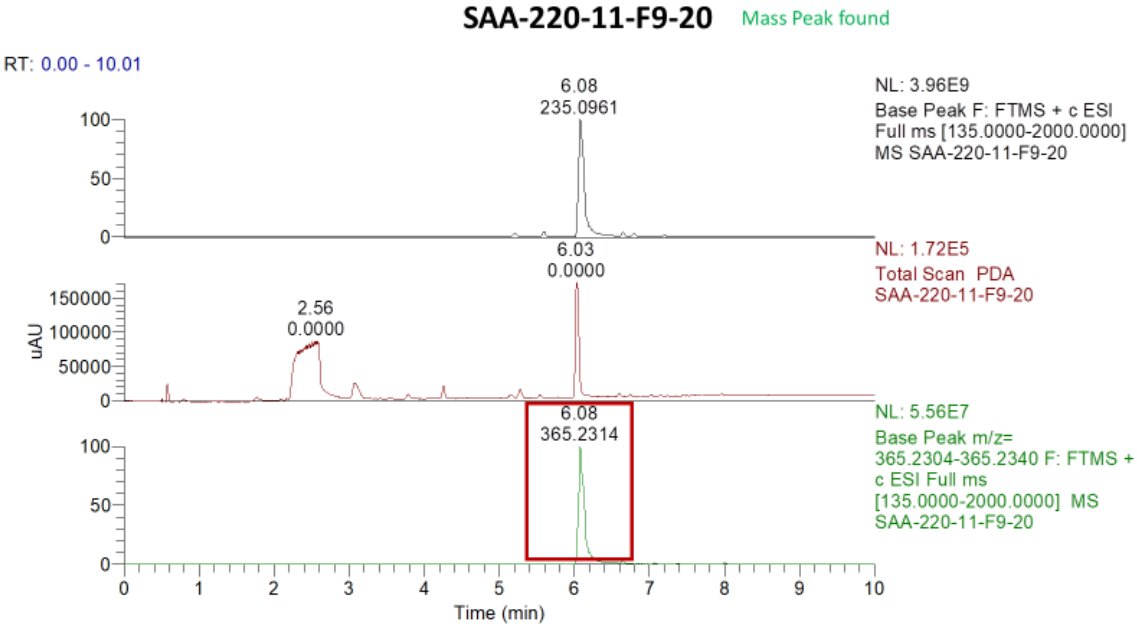
SAA-220-11-F9-20
Mass Peak found
RT: 0.00 - 10.01
6.08
235.0961
6.03
0.0000
2.56
0.0000
6.08
365.2314
uAU
Time (min)
NL: 3.96E9
Base Peak F: FTMS + c ESI Full ms [135.0000-2000.0000] MS SAA-220-11-F9-20
NL: 1.72E5
Total Scan PDA SAA-220-11-F9-20
NL: 5.56E7
Base Peak m/z= 365.2304-365.2340 F: FTMS + c ESI Full ms [135.0000-2000.0000] MS SAA-220-11-F9-20

SAA-220-25 Mass Peak found

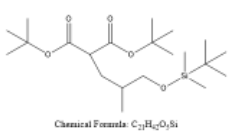

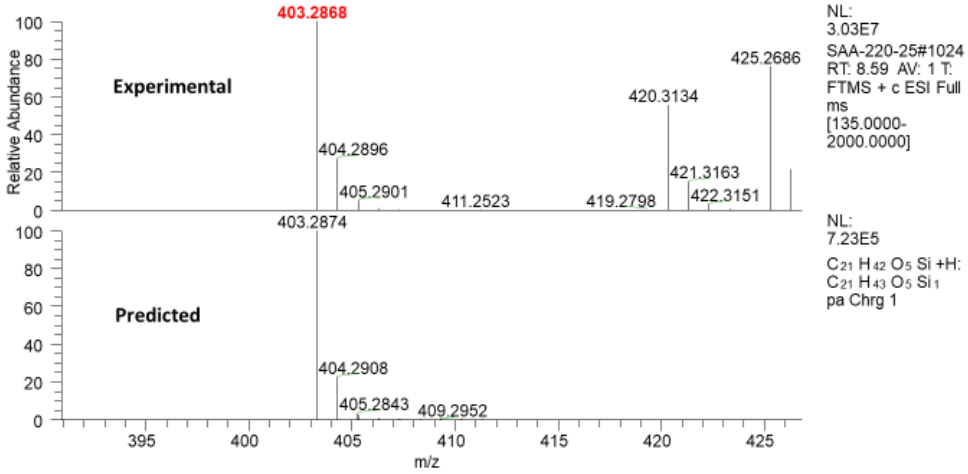

SAA-220-25 Mass Peak found

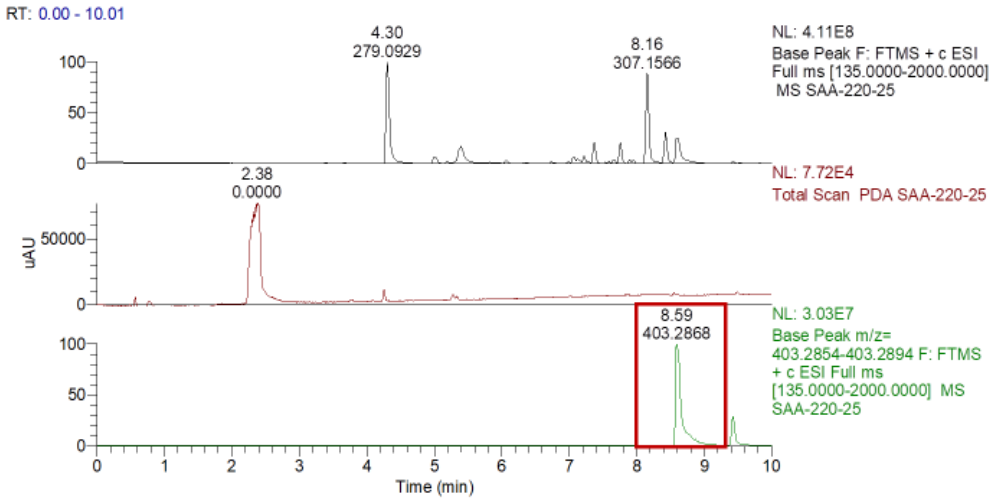

SAA-15F24

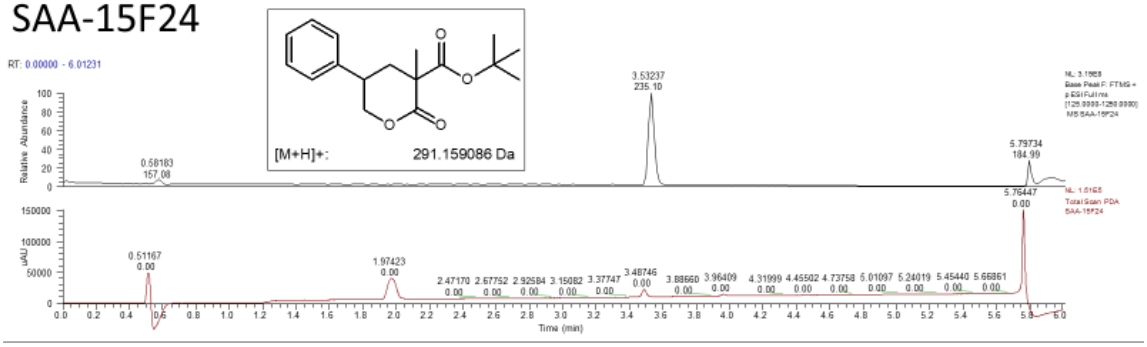
RT: 0.00000 - 6.01231
[M+H]+: 291.159086 Da
3.53237
235.10
0.58183
157.08
5.79734
184.99
5.76447
0.00
0.51167
0.00
1.97423
0.00
Relative Abundance
uAU
Time (min)

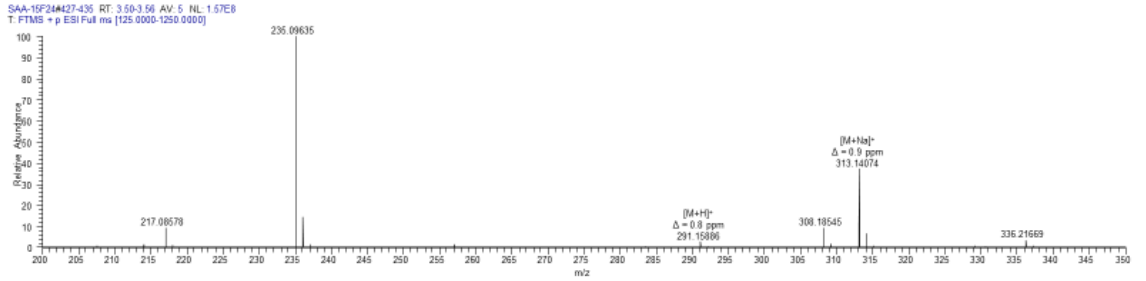
SAA-15F24#427-435 RT: 3.50-3.56 AV: 5 NL: 1.57E8
T: FTMS + p ESI Full ms [125.0000-1250.0000]
235.09635
[M+Na]+
Δ = 0.9 ppm
313.14074
[M+H]+
Δ = 0.8 ppm
291.15886
217.08578
308.18545
336.21669
Relative Abundance
m/z